Pharm Res (2011) 28:1500–1519
DOI 10.1007/s11095-010-0339-8

EXPERT REVIEW

Designing Dendrimers for Drug Delivery and Imaging: Pharmacokinetic Considerations

Wassana Wijagkanalan • Shigeru Kawakami • Mitsuru Hashida

Received: 29 July 2010 / Accepted: 29 November 2010 / Published online: 23 December 2010

ABSTRACT Dendrimers have well-organized high branches with a layered architecture providing a series of versatile chemical modification for various purposes. Consequently, this dendrimer nanotechnology explores a new promising class of nanoscale carriers for therapeutic drugs and imaging reagents using passive and active targeting approaches. By controlling dendritic structures, the biological fate of dendrimer/dendrimer-based drugs can be significantly altered based on their intrinsic physicochemical properties, including the hydrophilicity of the unit molecules, particle size, surface charge, and modification. Accordingly, pharmacokinetic aspects play an important role in the design and development of dendrimer systems for successful *in vivo* application and clinical translation. This review focuses on the recent progress regarding dendritic architectures, structure-related toxicity, and critical factors affecting the pharmacokinetics and biodistribution of dendrimer/dendrimer-based drugs. A better understanding of the basic aspects of dendritic systems and their pharmacokinetics will help to develop a rationale for the design of dendrimers for the controlled delivery of drugs and imaging reagents for therapeutic or diagnostic purposes.

KEY WORDS biodistribution · dendrimer · drug delivery · imaging · pharmacokinetics

W. Wijagkanalan (✉) • S. Kawakami • M. Hashida (✉)
Department of Drug Delivery Research
Graduate School of Pharmaceutical Sciences Kyoto University
46-29 Yoshida Shimoadachi-cho, Sakyo-ku
Kyoto 606-8501, Japan
e-mail: wwijagkanalan@gmail.com

W. Wijagkanalan
e-mail: ywassana@ddspharm.mbox.media.kyoto-u.ac.jp

M. Hashida
e-mail: hashidam@pharm.kyoto-u.ac.jp

W. Wijagkanalan
The Japan Society for the Promotion of Science (JSPS)
Chiyoda-ku Tokyo 102-8471, Japan

W. Wijagkanalan • M. Hashida
Institute of Integrated Cell-Material Sciences (iCeMS)
Kyoto University
Kyoto 606-8501, Japan

INTRODUCTION

Regarding the advance of polymer technology, the design of polymers for pharmaceutical application has been practically controlled by modifying the polymeric structure, size, topology and, ultimately, the physicochemical properties using polymer chemistry. This leads to a number of developments in polymer therapeutics, including polymeric drugs and micelles, which have not only been used in research field but also transferred to the clinic (1). The major polymeric therapeutic agents on the market or used in clinical trials are polymer–protein or –drug conjugates and polymeric micelles which are mainly based on polyethylene glycol (PEG) conjugation (PEGylation) and entrapment of drugs in micelles, respectively (1,2). These approaches demonstrate improvements in drug solubility, stability, and toxicity as well as a reduction in systemic clearance with enhanced permeability and retention (EPR) for effective cancer chemotherapy (1,3). Unfortunately, these polymers still present challenges as far as pharmaceutical development is concerned due to their intrinsic heterogeneity, which greatly influences their biological fate and activity, resulting in variability in therapeutic outcomes (1).

During the past several decades, highly branched spherical macromolecules have emerged due to the pio-

neering works of the Vogtle (4) Denkewalter (5), Tomalia (6) and Newkome (7) groups. This has been characterized as a new class of polymers which was first named a "cascade" molecule by Vogtle *et al.* (4) and later renamed as a "dendrimer" to emphasize the tree-like structure of larger dendritic molecules (5,6). Unlike conventional linear polymer and polymeric micelles, dendrimers can be prepared by controllable branched chemistry. Therefore, they possess a unique dendritic structure with attractive features, including their nano-size range, monodispersity, rigid globular structure with high physical stability, and a large number of peripheral functionality for versatile chemical modification (8). According to these unique advances, the emerging role of dendrimers in pharmaceutical fields has been highlighted by their extensive applications for therapeutic and diagnostic purposes, including the passive or active delivery of anticancer drugs (9), contrast agents (10) and nucleic acid drugs (11,12). As a general principle for designing dendrimers, there are many critical factors, such as their biocompatibility and pharmacokinetic characteristics, before dendrimer-based drugs can be used as biomedicines. The dendritic structure, modification and physicochemical properties of dendrimers have been reported in association with alterations in the toxicity and biodistribution of dendrimers and dendrimer-based drugs. These emphasize the importance of the systemic evaluation of structure-related pharmacokinetics to fully assess any pharmacodynamic interactions.

In this review, we relate the dendritic structure, chemical modification and physicochemical properties of dendrimers to biocompatibility and pharmacokinetic considerations, including biodistribution and excretion data, based on recent advances. More broadly, the future prospects based on pharmacokinetic aspects are discussed to develop a rationale for the design of dendrimers, allowing the controlled delivery of drugs and imaging reagents for therapeutic or diagnostic purposes.

DENDRITIC ARCHITECTURE

Composition

Dendrimers, consisting of a central core, internal cavity (void space) and peripheral groups, are well-defined and highly branched macromolecules which govern globular structure with monodispersity (6) (Fig. 1a). Dendrimers are generally synthesized stepwise using divergent or convergent methods. Regarding the divergent method first developed by the Tomalia (6) and Newkome (7) groups, dendrimers grow exponentially outwards by conjugation of repeated branch units to the end groups of the central core. On the other hand, the Frechet groups demonstrated a convergent synthesis starting from the periphery of dendrimers toward the central core in which this part is termed "dendron" and finally linking to the core molecule to introduce a complete dendrimer (13). The degree of branching is dictated by the multiplicity of the central core, while the dendritic structure of branch units is characterized in a layer defined as generation (G) in which the central core is sometimes referred to as generation zero (G0). The higher the generation the larger the particle size, the larger internal cavity, the higher the peripheral groups, the more rigid the structure (Fig. 1a and Table I). Generally, a theoretically monodisperse dendrimer size can be obtained by both synthetic methods. However, a perfectly dendritic structure of a higher generation dendrimer could be successfully prepared by the convergent method due to the lower steric hindrance of the crowded peripheral groups during synthesis (14). Besides the central core and internal cavity, the peripheral groups on the surface of dendrimers crucially determine the overall physicochemical properties of dendrimers, such as their solubility, charge, hydrophobicity, and hydrophilicity. These properties have been reported to be closely associated with biocompatibility, biodistribution, and pharmacokinetic characteristics (15–18), as will be discussed in this review. A vast number of dendrimers have been designed with structural difference used in biological applications, including polyamidoamines (PAMAM) (6), polypropyleneimines (PPI) (19), polyamides or polypeptides (20), polyester (21), and polymelamine (22) dendrimers. Recently, polytriazole dendrimers synthesized by "click chemistry" (23) and "geometrically disassembling" or degradable dendrimers have been developed for controllable structure cleavage by light, enzymes or single triggering events (24). This is a new concept in dendrimer chemistry for improved biological applications although these approaches are still in their infancy. By varying the central core (i.e. ammonia (AC), ethylenediamine (EDA)) and peripheral groups (i.e. amine, carboxylate, hydroxyl, succinate), commercially available PAMAM (Starburst™) and PPI dendrimers has been widely used for therapeutic and diagnostic purposes. In addition, polypeptides or amino acid lysine dendrimers have been recently developed as biodegradable dendrimers for potentially safer pharmaceutical vehicles for future clinical applications (25). The literature reports discussed in this review are mainly based on the investigation of these dendrimers (Fig. 1b-c).

Structure-related Toxicity

Toxicity evaluation is extremely important for the development of nanomaterials, including polymers and dendrimers, which will be used clinically. The toxicity of polymers is a complex issue involving the molecular function and physico-

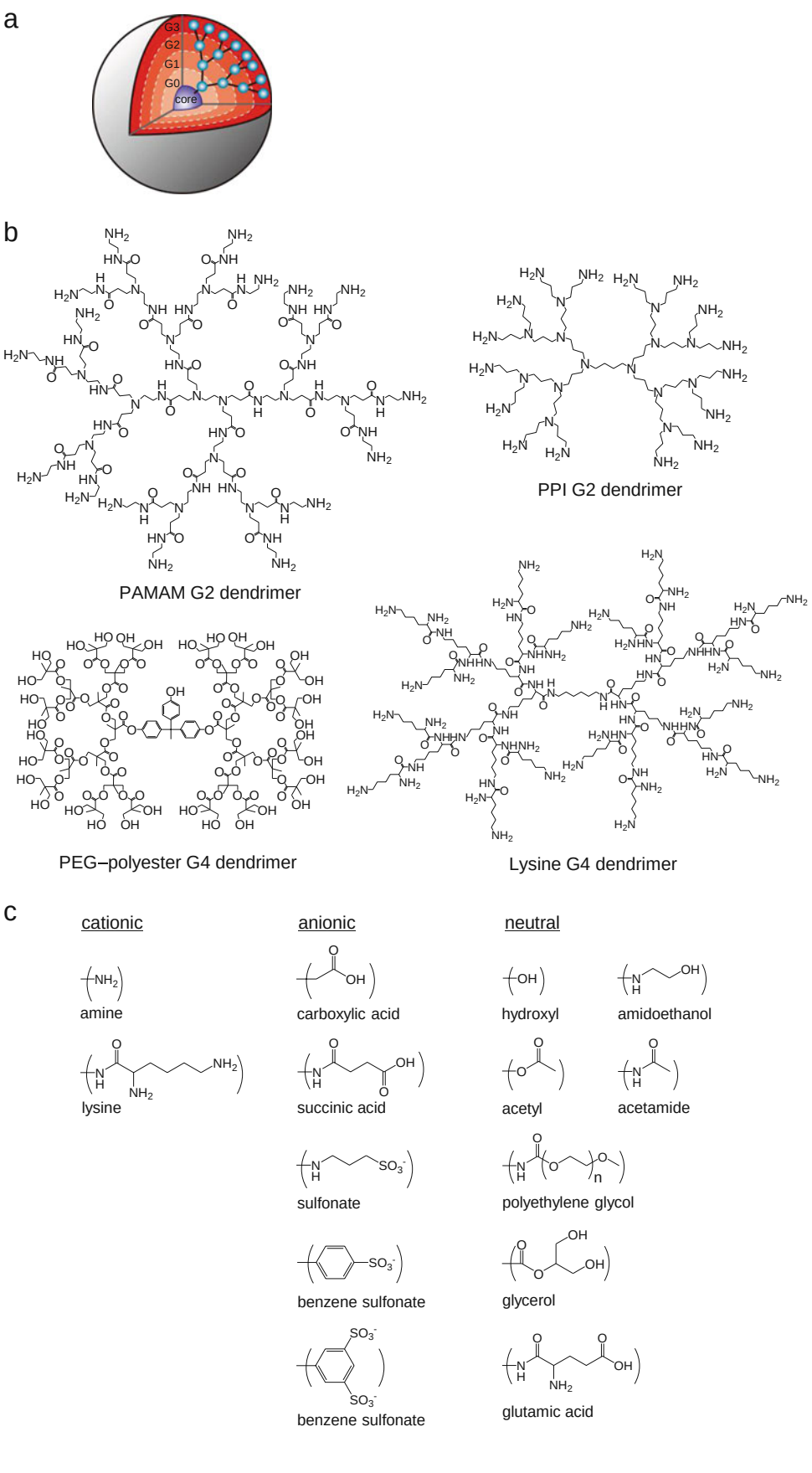

Fig. 1 (**a**) Dendritic architecture (adapted from (8,18), (**b**) Various types of dendrimers used in biomedical application (19,41,43,44), and (**c**) their peripheral groups classified by charge.

Table I Characteristics of PAMAM Dendrimers with Ammonia Core

Generation	MW	Number of surface groups	Hydrodynamic diameter (Å)[a]	Hydrodynamic volume (ml $mol^{-1} \times 10^{-21}$)[b]
1	1043	6	15.8	0.761
2	2411	12	22.0	2.55
3	5147	24	31.0	7.66
4	10619	48	40.0	19.1
5	21563	96	53.0	63.1
6	43451	192	67.0	–
7	87227	384	80.0	–

Data from (6,44)

[a] Determined by size exclusion chromatography

[b] Determined in methanol

chemical nature of polymers, route of administration, dose, biodistribution characteristics, and physiological interaction (26). Although an *in vitro* test can suggest potential toxicity, it is not directly related to the *in vivo* effect. Accordingly, Duncan and colleagues have developed a series of *in vitro* and *in vivo* toxicity tests as a screening step before preclinical assessment studies (16). The *in vitro* screening (MTT assay) is commonly performed by cytotoxicity testing in a panel of cells. More *in vivo*-related assays have been established using a hematocompatibility assay (lysis of red blood cells and complementary activation), and a polymer biodegradation test. Short- and long-term biodistribution studies as well as the immune response and metabolic fate of polymers are important criteria for evaluation of *in vivo* toxicity. Since the *in vivo* toxicity of polymers is a consequence of their high deposition in tissues or organs, this highlights the tissue/organ-specific toxicity and toxicokinetic aspects which will be discussed based on the pharmacokinetic and biodistribution viewpoint in the following section.

The potential toxicity of dendrimers has been extensively studied using the *in vitro* MTT assays and permeability in a number of cell lines. Despite differences in cell types and experimental conditions, the general toxicity of dendrimers is defined in a surface charge-, generation-, and concentration-dependent manner. Roberts *et al.* showed that cationic PAMAM G7 dendrimers exhibited less than a 10% cell viability in Chinese hamster lung fibroblast V79 cells at 100 nM compared with G5 dendrimers at 10 μM and G3 dendrimers at 1 mM, which was irrespective of the exposure times of 4 and 24 h (27). An extended study was reported by Malik *et al.* using a variety of dendrimer types (PAMAM, PPI with a diaminobutane (DAB) and a diaminoethane (DAE) core, carbosilane–polyethyleneoxide (CSi–PEO)), surface molecules (amine, carboxylate), and different generations (G1–4) (28). Cationic dendrimers were cytotoxic to B16F10 cells (IC_{50} = 50–300 μg/ml) and produced hemolysis (at 1 mg/ml) in a generation-dependent manner corresponding to the effect of lysine dendrimers (29). Surprisingly, cationic PAMAM dendrimers were less toxic than cationic DAB– and DAE–PPI dendrimers having an equal number of surface amine groups. In contrast, anionic and neutral dendrimers produced much less hemolysis than their cationic counterparts; however, enhanced toxicity was observed by the lower generation of CSi–PEO dendrimers, suggesting greater accessibility of the potentially toxic central core to the cells (28). Hong *et al.* reported the cytotoxic mechanism of cationic dendrimers on the integrity of cell membranes using a lipid bilayer membrane model and cell cultures (30). Cationic PAMAM dendrimers induced a loss of cell integrity determined by the release of the enzyme lactodehydrogenase and pore-formation (15–40 nm in diameter) in a lipid bilayer model involving generation dependence.

To overcome structure-induced cytotoxicity, many approaches have been developed based on the suppression of the cationic surface by PEGylation, acetylation, and modification with anionic, neutral, and ligand molecules. PEGylation, using PEG MW 2–5 kDa, of cationic PAMAM dendrimers significantly reduced the toxicity in a number of cells, including Caco-2 cells (31), endothelial cells (32), and hemolysis (33) compared with the unmodified counterparts. In addition, Kolhatkar *et al.* demonstrated that acetylation or amidation of amine groups on the PAMAM surface led to ten-fold lower cytotoxicity without loss of permeability across Caco-2 cells (34). Interestingly, folate-conjugated or folate-acetylated (Ac) PAMAM dendrimers produced less hemolysis and *in vivo* gross toxicity, respectively (35,36). These findings support the linear relationship between the cationic charge density on dendrimers and cytotoxicity. Recently, the Szoka groups demonstrated the low cytotoxicity of neutral surface- or PEG–polyester dendrimers, irrespective of their size, in MDA-MB-231 cells (37,38). Interestingly, Hashida and colleagues reported a new approach to reduce the cytotoxicity of lysine G6 dendrimers by surface modification with glutamic acid, called KG6E dendrimers (39). The glutamate residues having an equal number of amines and carboxylates could maintain chemical functionality while compromising cytotoxicity compared with cationic PAMAM G5 dendrimers.

Similar to the *in vitro* toxicity, cationic polymelamine dendrimers induced subchronic liver toxicity by increasing the serum alanine transaminase level after intraperitoneal

injection of 10 mg/kg (40) correlated to the dose-dependent release of this enzyme following intravenous injection of lysine and PAMAM G6 dendrimers (41). Increasing the dose to 160 mg/kg led to acute liver necrosis and mortality 12 h post-injection (40). On the other hand, PEGylated cationic polymelamine (42) and PEG–polyester dendrimers (43) were very well tolerated in mice after intraperitoneal or intravenous administration at a dose of 1 g/kg.

Dendritic Vehicles for Therapeutic Drugs and Imaging Reagents

The dendrimer generations 4–6 (10–50 kDa, 4–7 nm in diameter), despite slight differences in each type of dendrimer, have been exploited as suitable vehicles for biological application due to synthesis reproducibility, adequate internal cavity and peripheral functionality, controllable biodistribution, and acceptable cost (18,44). According to the flexibility of the chemical modification, hydrophobic cavity and positive surface potentials, dendrimers offer a platform for high payload drugs or imaging reagents for efficient passive delivery by PEGylation (45–47) and active targeting using folate (36,48,49), antibody (39,50,51) and sugar moieties (52). Dendrimers have widely been used as delivery vehicles for anticancer or nucleic acid drugs, which is not limited to conjugation or complexation at the periphery but also involves encapsulation in the internal cavity.

Dendrimer conjugation of anticancer drugs, including methotrexate (53–55), doxorubicin (56–59), and camptothecin (60), and imaging reagents (i.e. gadolidium (Gd)) (10,61) can provide a high payload which results in the reduction of the administered dose for minimizing side-effects, maximizing therapeutic outcomes, and improving contrast property. The application of dendrimers for magnetic resonance imaging (MRI) was first demonstrated by Wiener *et al.* using Gd-radiolabeling PAMAM dendrimers (PAMAM–Gd) with a DTPA chelate (61). The high multiplicity of Gd–DTPA on PAMAM dendrimers increases the longitudinal relaxation giving higher signal intensity in the surrounding tissue. Furthermore, dendrimer conjugation may increase the complex stability of Gd–DTPA, exhibit intravascular retention and reduce renal toxicity, which can be observed in free Gd–DTPA (Magnevist®). As will be discussed later, the dendritic structure allows changes of the signal intensity and organ-specific imaging of dendrimer-based Gd, and this has been extensively studied by Kobayashi and colleagues (10). In addition, tumor imaging with a targeting ligand using folate-conjugated PAMAM–Gd showed a contrast signal in tumor tissue for 24 h, while free Gd–DTPA exhibited a short half-life of 20 min after injection in tumor-bearing mice (62). The tumor targeting of dendrimer-based drugs has been well-documented using FDA-approved antibodies, such as trastuzumab (39,51,54) and cetuximab (63,64), against epidermal growth factor HER2 and EGF receptors, respectively. Recently, trastuzumab conjugation to anionic amino acid KG6E dendrimers or PAMAM-Ac dendrimers has been used as an effective targeting system for HER2-overexpressing breast cancer cells with less non-specific interactions *in vitro* (39,51,54). Furthermore, methotrexate-conjugated trastuzumab-cationic PAMAM dendrimers exhibited anticancer activity after tumor uptake, despite having only a modest effect compared with anionic PAMAM conjugation (53). The low activity of methotrexate-conjugated cationic PAMAM dendrimers was due to the brief retention of cationic dendrimers in lysosomes resulting in insufficient drug release (53,65). This emphasizes the great impact of the cleavable linker and dendrimer properties on drug release. A tailored drug release has been proposed for effective drug release at the target site using cleavable linkers. Most of the attention has been directed towards the cleaving process in lysosomes or the cellular environment of hydrolytic esters (54), amides (53,66) with glycine spacer (60), pH-sensitive hydrazones (43,56,57), and reducible disulfides (67). Najlah *et al.* directly compared the release of ester- and amide-linked conjugates of naproxen to PAMAM G0 dendrimers in 80% human plasma and liver homogenate (66). An amide-linked naproxen exhibited a poor release, whereas the ester linkage was rapidly hydrolyzed by esterases to produce drug release with a half-life of almost 1 h. As reported by Szoka and colleagues, doxorubicin-functionalized bow-tie (56,57) and PEG–polyester dendrimers (43) with a hydrazone linkage have been shown to be a very effective cure for cancer *in vivo* and *in vitro*, respectively. This was suggested to be due to the cleavage of the hydrazone at a low pH in the lysosomes. In addition, the reducible disulfide linking system has been developed by the Kannan group to attach *N*-acetyl cysteine (anti-oxidant and anti-inflammatory agent) to cationic PAMAM dendrimers for the treatment of inflammation (67). The cleavage of the disulfide bond was triggered by a disulfide exchange reaction with intracellular, rather than plasma, glutathione for rapid release of *N*-acetyl cysteine for a 16-fold increased anti-oxidative efficacy in activated microglial cells.

Another role of the dendritic vehicle is the encapsulation in the dendritic cavity for improved solubility and increased payload of poorly water-soluble drugs (i.e. anticancer and anti-inflammatory agents) (17,44). Unlike micelles, dendrimers are thermodynamically stable, so they, are sometimes referred to as "unimolecular micelles" or "dendritic box" for drug encapsulation that can be used as promising drug vehicles in host-guest chemistry (8,68). The mechanism has been proposed to be a hydrophobic interaction involving hydrogen bonding, a π-π interaction

of the encapsulated drugs and the internal cavity of the dendrimers or the electrostatic complexation of positive and negative charges on the dendritic periphery and drug molecules *per se* (69). The encapsulation efficiency has been suggested for generation-dependent fashion observed by incorporation of phenobarbital in PAMAM (G3–6) (70), paclitaxel in polyglycerol (G3–G5) (71), and methotrexate in polyester-co-polyether (dendrimer series G1–G2) (72) dendrimers. The higher generations of polyester-co-polyether series 2 dendrimers provided a relatively slower release profile with lower burst release (72). The larger internal cavity and denser periphery of the higher generation dendrimers is more capable of increasing the drug encapsulation and potentially prolonging the drug release. PEGylation of dendrimers has been shown to enhance solubilization (45) and improve release profile due to steric hindrance (71). Kojima *et al.* demonstrated that the increased encapsulation of methotrexate and paclitaxel in PEG–PAMAM dendrimers was in parallel to the higher generations of PAMAM and molecular mass of PEG. However, PEG with high MW of 5 kDa reduced the drug encapsulation due to the agglomeration of the PEG chain occupying the dendritic cavity available for drug molecules (45,73). Similar to the PEG effect, surface modification of PPI (74) and PAMAM G4 (49) dendrimers with mannose and folate resulted in a slower release of encapsulated lamivudine and indomethacin, respectively. The effective therapy of dendrimer-encapsulated drugs has been extensively studied *in vitro* (75), but only a few *in vivo* studies have been done. Malik *et al.* first investigated the *in vivo* application of PAMAM-complexed cisplatin for cancer treatment after intravenous administration (76). The high tumor accumulation of cisplatin delivered by PAMAM dendrimers, rather than free drug, significantly suppressed the tumor growth in a solid tumor mouse model, indicating a successful EPR effect for drug release at the tumor site. Subsequently, *in vivo* studies of non-covalently bound anti-inflammatory drugs in cationic PAMAM dendrimers have produced good results; however, the premature or rapid release before reaching the target site is still problem for clinical use (17,35,49,77).

Considering the role of dendrimers in drug delivery, a direct comparison of the effectiveness of dendrimer-conjugated or encapsulated methotrexate was clearly reported by Baker and colleagues (78). Conjugated methotrexate exhibited higher anticancer activity with lower systemic toxicity, whereas its encapsulated counterpart had a similar effect to the free drug, which might be caused by the premature release of methotrexate after administration. Dendrimer-conjugated drugs with tailored drug release effect have been suggested as a superior delivery system. Nevertheless, there is a need for optimization of the dendrimer-drug system not only by conjugation but also by noncovalent interaction to obtain a suitable release profile at the target site by linker chemistry, modification with PEG or targeting ligands, and the administration route of choice (8,17,24).

The role of dendrimers as a non-viral vector gene transfecting agent has been established based on the positive surface charge for complexation with the phosphate backbone of DNA which has been reported by many groups. The transfection efficiency using dendrimers, such as PAMAM (79), and lysine dendrimers (80) is sometimes difficult to achieve since the number of positive charges and the size or generation of dendrimers critically affect DNA binding or complexation (81), aggregation (79), cytotoxicity (29) and, ultimately, gene expression level (80,82), which is discussed in other reviews (12).

GENERAL PHARMACOKINETICS AND BIODISTRIBUTION

The fundamental pharmacokinetics and biodistribution are principally based on anatomical and physiological characteristics, the physicochemical properties of macromolecules and their interactions (83,84). In a simple model, such as intravenous administration, macromolecules are immediately introduced into the blood circulation with restricted diffusion to the extravascular space. Then, the circulating macromolecules are eliminated from the blood pool and distributed to particular organs for disposition, which reflects the plasma clearance by these organs or tissues. Based on the clearance concept, the tissue distribution of macromolecules in linear pharmacokinetic model can be characterized by tissue uptake; this clearance is assumed to be independent of their plasma concentration, and their efflux from tissue is very low (83). For the active targeted macromolecules with saturated uptake process, the tissue uptake clearance depends on their plasma concentration following non-liner Michaelis-Menten kinetics with limited maximum clearance. In general, the specific tissue uptake of macromolecules critically depends upon the organ blood flow, capillary permeability and nature of the macromolecules. Macromolecules with a molecular weight less than 30–50 kDa or a diameter of 5–6 nm, such as recombinant human superoxide dismutase (SOD) (MW 32 kDa), easily enter into the glomerular capillaries of the kidney and undergo glomerular filtration, then excrete into the urine (84,85). The larger macromolecules are trapped in the liver by passing through the hepatic fenestrae with a pore size of about 100 nm (86). The positively charged macromolecules, including cationized bovine serum albumin (cat-BSA) (MW 70 kDa) and SOD (cat-SOD) (MW 34 kDa),

are electrostatically adsorbed to the negatively charged cellular surface in most organs, especially kidney (85,87) and liver (88). Because of a high hepatic blood flow and many fenestraes for direct interaction with liver cells (86), cationic macromolecules predominantly accumulate in the liver parenchymal cells (88), whereas polyanionic molecules, such as succinic-modified BSA (suc–BSA) (MW 70 kDa), are selectively taken up by liver nonparenchymal cells via scavenger receptors (89). In some cases of active targeting, such as galactosylated BSA, this protein is extensively taken up via galactose receptors upon entering the liver and exhibit a high hepatic clearance identical to the hepatic plasma flow rate (85000 μL/h), which is considered as a maximum hepatic clearance of this protein in mice. The target-specific clearance of targeted macromolecules might not solely involve a high affinity of ligand-receptor interaction but also a balance of the aforementioned physicochemical properties and administered dose with the receptor-triggered clearance becoming saturated at a high dose (84). In addition, larger macromolecules with neutral or weak anionic charges or hydrophilicity, including BSA (MW 67 kDa) or immunoglobulin (IgG) (MW 150 kDa), potentially escape from opsonization for uptake by the reticuloendothelial system (RES) (i.e. liver and spleen), resulting in a prolonged blood circulation with a high area under the curve (AUC) (90). This phenomenon suggests that the neutral or anionic surface charge of the designed dendrimers reduces the nonspecific interaction or opsonization for the desired plasma profiles. Figure 2 summarizes the relationship between the disposition characteristics and general physicochemical properties of macromolecules based on the clearance concept.

For the use of macromolecule-conjugated drugs, the release kinetics of drugs from macromolecules are a second important issue to evaluate the effectiveness of delivery systems for therapeutic purposes in the intended target tissue such as tumor tissue (15,83). Unlike those of nonconvalent encapsulation with a burst effect, the release kinetics of conjugated drugs commonly follow first-order kinetic process with respect to drug concentration, the rate of which is a function of drug concentration and markedly affected by the nature of the linkers and the microenvironment conditions. The ester-linked drugs, such as camptothecin–PEG–lysine (60) and naproxen–PAMAM (66) dendrimers, are more rapidly cleaved in physiological condition compared to other linkages (66,91). This process is more susceptible for nonenzymatic hydrolysis, since enzyme may hardly access due to steric hindrance of crowded dendrimer surface (60,91). The enzyme-triggered drug release is dependent on the dendrimer structure for enzyme access, the concentration of dendrimer-linked drugs and enzymes in Michealis-Menten kinetic model. However, the *in vivo* drug release studies at the target site are very difficult to carry out. At this site, the released drugs exhibit pharmacological actions depending on their concentration. The effectiveness of macromolecule-

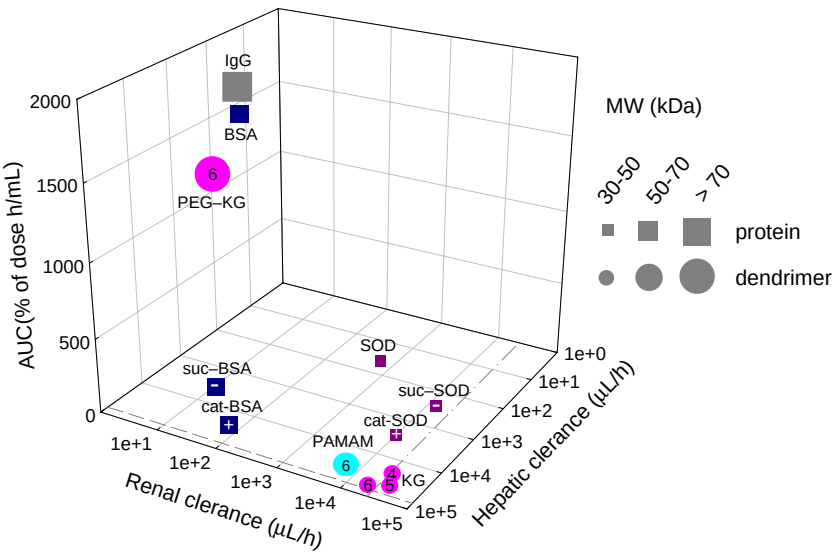

Fig. 2 The relationship between physicochemical properties (MW and charge) and pharmacokinetic parameters (AUC, hepatic and renal clearance) of proteins (rectangular) and dendrimers (circle) after intravenous administration in mice. The maximal hepatic and renal clearance are predicted by hepatic plasma flow rate (dash line) and glomerular filtration rate (dash-dot line). IgG; bovine immunoglobulin G, BSA; bovine serum albumin, cat-BSA; cationized BSA, suc–BSA; succinylated BSA, SOD; recombinant human superoxide dismutase, cat-SOD; cationized SOD, suc–SOD; succinylated SOD, KG; lysine dendrimers, PEG–KG; PEGylated lysine dendrimers, PAMAM; polyamidoamine dendrimers. +; cationic, −; anionic, number inserted in symbols; the generations of dendrimers. (Adapted from (41,83,84,89) and unpublished data).

conjugated drugs compared with free drugs can be evaluated in term of therapeutic availability (TA) based on the total drug amount as a function of the AUC at the target site (92). In the case of no redistribution of released drug from the target site, the TA value could be predicted by the tissue uptake clearance parameters. The pharmacological response produced as a consequent effect of released drugs is one of the main pharmacodynamic parameters which is closely related to the release kinetics. Although the *in vivo* release kinetics are pharmacodynamically important, it might be possible to ignore them when the drug could pharmacologically function in conjugated form (54,93) or if there was rapid release of the noncovalently bound drug from macromolecules (35,49,77). Based on these assumptions, the *in vivo* release kinetics might alternatively be estimated by a pharmacological activity ratio, tissue uptake clearance, and other pharmacokinetic parameters. These values in some literature reports have been discussed and summarized in Tables II and III.

FACTORS AFFECTING THE BIODISTRIBUTION AND PHARMACOKINETICS OF DENDRIMER/ DENDRIMER-BASED DRUGS

Ideally, dendrimers are developed to deliver drugs to target tissues to obtain sufficient therapeutic efficacy and avoid toxic effects on the healthy bystander cells which are associated with the potential organ-specific toxicity of the free drugs. This could be accomplished by optimization of the biodistribution characteristics of dendrimers. A large number of biodistribution and pharmacokinetic studies have mainly used empty dendrimers. However, the surface conjugation of drugs or labeling probes in dendrimer-based drugs may significantly change the overall properties of dendrimers resulting in different pharmacokinetic profiles from the dendrimer itself (43,94). The metabolic products of dendrimer-based drugs, such as a dendrimer fragment and free drug, could be involved in the redistribution at a later time (25,95). It is of paramount importance to carefully investigate the biodistribution and pharmacokinetics of the empty dendrimer and dendrimer-based drug in parallel.

The biodistribution and pharmacokinetics of dendrimers were systematically studied using a series of PAMAM, DAB–PPI, PEG–polyester and lysine dendrimers with different physicochemical properties, including the central core, peripheral groups, charge, hydrophilicity, hydrophobicity, and surface modification. The following discussion summarizes the biological disposition and pharmacokinetic parameters of dendrimers to obtain a generalization helpful for the design of dendrimers for drug delivery (Table II) and imaging (Table III); however, some variables are unavoidable due to differences in experimental methods.

Size and Generation

Since the size and charge act in concert to influence the whole body distribution of dendrimers, it is sometimes difficult to identify the distinct effect of these factors on different types of dendrimers even using a similar experimental design (27,96,97). A series of works reported by Kobayashi and colleagues came to a conclusion about the effect of size or generation on the biodistribution characteristics of dendrimers using MRI analysis (98,99). Cationic PAMAM dendrimers with EDA and AC cores, G1–10 (MW 1–935 kDa, 1–15 nm in diameter) were conjugated with a bifunctional DTPA derivative (1B4M) as a chelator for Gd. Almost 100% 1B4M modification was obtained to yield saturated ^{153}Gd-radiolabeling PAMAM dendrimers (PAMAM–Gd) with an overall negative surface charge and increased MW (MW 7–3820 kDa for G1–10) compared with the unmodified counterparts (10). After intravenous injection in mice, PAMAM–Gd was rapidly cleared from the blood circulation and mainly distributed to the liver, spleen and kidney by means of their size. Increased generation resulted in prolonged blood retention and reduced renal excretion as demonstrated with PAMAM–Gd G5–8 (MW 88–954 kDa) in a corresponding MRI angiography study (98,99). However, too high a generation is unlikely to increase the blood retention since the RES (liver and spleen) can recognize the larger particles, such as PAMAM–Gd G9, for rapid elimination from the blood pool (99,100). This is in agreement with the theoretical MW cutoff of glomerular filtration for rapid renal excretion of PAMAM–Gd G2–4 with a MW range of 15–59 kDa (10,98). Interestingly, PAMAM–Gd G5 underwent partial filtration (~59% of dose/g) even though it had a higher MW (88 kDa) than the MW cutoff for glomerular filtration. Importantly, the more compact the structure of dendrimers than nonspherical proteins or linear macromolecules at the same MW could account for this observation (85,98,101). The biphasic blood clearance profiles showed a higher distribution half-life of the α (5–13 min) and β elimination (~1 h) phase for dendrimers G5–8. However, the elimination half-life of Gd–DTPA and PAMAM–Gd G3 was significantly higher due to their smaller size (1–3 nm) for ready extravasation to the surrounding tissue, resulting in a high background in the MRI images (98). Accordingly, PAMAM–Gd G6 might be the smallest generation for low renal excretion (~15% of dose/g) with restricted blood retention indicating that G6–8 were optimal for vascular imaging (98,99). Interestingly, the function of a high generation is more pronounced in the tumor microvasculature of a solid tumor mouse model,

Table II Dendrimers for Drug Delivery and Their Therapeutic Availability (TA)

Application	Model	Active agent	Dendrimer	Interaction (linkage)	TA[a]	Ref.
Anticancer						
1. *In vitro* cytotoxicity	MTX-sensitive cells MTX-resistant cells	Methotrexate	PAMAM-G2.5-COOH	Conjugation (amide)	1–3 8–24	(53)
2. Intravenous	KB solid tumor mice	Methotrexate	Folate-PAMAM-G5-Ac	Conjugation (amide)	4.5[b]	(36)
	C26 solid tumor mice	Doxorubicin	Bow-tie polyester	Conjugation (hydrazone)	9	(56)
	C26 solid tumor mice	Doxorubicin	PEG-polyester	Conjugation (hydrazone)	~14	(57)
	C26 solid tumor mice	Camptothecin	PEG-lysine G2	Conjugation (glycine-ester)	14.5	(60)
	B16 solid tumor mice	Doxorubicin	PEG-PAMAM-G4	Conjugation (*cis*-aconityl)	38	(115)
	Healthy rats	5-fluorouracil	PEG-PAMAM-G4	Encapsulation	0.71	(33)
3. Intraperitoneal	24JK-FBP solid tumor mice	Boron	Folate-PEG-PAMAM-G3-Ac	Conjugation (amide)	>6[b]	(48)
	SHIN3 peritoneal disseminated mice	Gadolinium	Avidin-PAMAM-G4-1B4M	Complexation	366 3.4[b]	(130)
	LM3 solid tumor mice	5-Aminolaevulinic acid	Propionamido carbamino benzene dendrimer G2	Conjugation (ester)	more sustained	(157)
4. Intratumoral	$F98_{EGFR}$ intracerebral tumor rats	Boron	EGF-PAMAM-G4	Conjugation	73 2180[c]	(50)
5. Oral	Healthy rats	Doxorubicin	PAMAM-G4-NH_2	Complexation	317[d]	(148)
Anti-inflammatory therapy						
1. *In vitro*	LPS-stimulated microgial cells	*N*-Acetyl cysteine	PAMAM-G4-NH_2	Conjugation (disulfide)	3–4	(67)
2. Intravenous	Carrageenan-induced paw edemic rats	Flurbiprofen	PAMAM-G4-NH_2	Complexation	1–1.8	(35)
	Adjuvant-induced arthritic rats	Indomethacin	PAMAM-G4-NH_2	Complexation	2–3 1.9[d]	(158)
3. Intraperitoneal	Adjuvant-induced arthritic rats	Indomethacin	Folate-PAMAM-G4-NH_2	Complexation	3–4 1.5–2[b]	(49)
	Various arthritic rat models	–	PAMAM-G4-NH_2 PAMAM-G4-OH	–	2.3–2.7	(159)
4. Transdermal	Carrageenan-induced paw edemic rats	Indomethacin	PAMAM-G4-NH_2 PAMAM-G4-OH	Complexation Encapsulation	2–2.4[d]	(77)
	Healthy rats	Ketoprofen Difuinisal	PAMAM-G5-NH_2	Complexation	2.7[d] 2.5[d]	(160)
Anti-thrombotic therapy						
1. Intratracheal	Healthy rats	Enoxaparin (0.5–1%)	PAMAM-G2 or G3-NH_2	Complexation	2–2.2	(140)
Miotic and Mydriatic activity						
1. Ocular	Healthy rabbits	Pilocarpine nitrate or tropicamide	PAMAM-G1.5-COOH PAMAM-G4-NH_2 PAMAM-G4-OH	Encapsulation	1.1–1.6	(161)
Antimararial therapy						
1. Intravenous	Healthy rats	Chloroquine phosphate	Chondroitin coated lysine-PEG-G5	Encapsulation	1.6[e]	(162)

[a] The ratio of total drug amount or drug activity of dendrimer–drug to free drug in the target tissue

[b] The ratio of total drug amount in ligand-modified to unmodified dendrimers in the target tissue

[c] The ratio of total amount of dendrimer–drug in the target tissue following non-intravenous to intravenous administration

[d] The ratio of total drug amount of dendrimer–drug to free drug in plasma

[e] The ratio of plasma drug concentration of dendrimer–drug by intravenous to free drug by intramuscular injection

Table III Dendrimers for Imaging

Application	Imaging agent	Dendrimer (route of administration)	Accumulation ratio[a]	Signal/ Noise ratio[b]	Ref.
1. Sentinel lymph node	$(1B4M\text{-}Gd)_{64}$ MRI	PAMAM-EDA-G4 (intracutaneous)	–	3	(103)
	$(1B4M\text{-}Gd)_{256}$ MRI	PAMAM-EDA-G6 (subdermal)	increased	3	(104)
	$(1B4M\text{-}Gd)_{128}$ MRI	PPI-DAB-G5 (intracutaneous)	–	4–5	(103)
	$(1B4M\text{-}Gd)_{191}$ and $(Cy5.5)_2$ Dual MRI and fluorescence	PAMAM-EDA-G6 (direct injection to mammalian glands)	–	increased	(163)
2. Lymphatic vessel (normal and metastatic/inflamed lymph vessles)	$(1B4M\text{-}Gd)_{1024}$ MRI	PAMAM-EDA-G8 (intracutaneous)	–	increased	(103)
3. Blood vessel	$(1B4M\text{-}Gd)_{192}$ MRI	PAMAM-AC-G6 (intravenous)	7	–	(98)
	$(1B4M\text{-}Gd)_{512}$ MRI	PAMAM-EDA-G7 (intravenous)	18	4–5	(99)
	$(1B4M\text{-}Gd)_{62}$ MRI	PEG_2-PAMAM-EDA-G4 (intravenous)	7	4–4.5	(114)
4. Tumor	^{99m}Tc PET	Porphyrin dendrimer (intravenous)	–	8–10	(164)
	$(DTPA\text{-}^{99m}Tc)_8$ SPECT	Folate-PEG-PAMAM-G5 (intravenous)	2.3	increased	(165)
	$(DTPA\text{-}Gd)_{30\text{-}60}$ and Rhodamine B_{22} Dual MRI and fluorescence	PAMAM G4-5 (intravenous)	increased	–	(166)
5. Tumor blood vessel	$(1B4M\text{-}Gd)_{1024}$ MRI	PAMAM-EDA-G8 (intravenous)	13	3–5	(99)
6. Angiogenesis (ischemic model)	$(^{76}Br)_8$ PET	cRGD-PEG-dendrimer (intravenous)	2–2.5	2.5–4	(133)
7. Liver	$(1B4M\text{-}Gd)_{64}$ MRI	PPI-DAB-G4 (intravenous)	37	2.5	(105)
	$(1B4M\text{-}Gd)_{2048}$ MRI	PAMAM-EDA-G9 (intravenous)	21	2–2.5	(99)

[a] Calculated from the concentration ratio of dendrimer-conjugated probe to free probe at the target site

[b] Determined by the signal intensity ratio of target to adjacent muscle tissues

which reflects the EPR effect (99). Although PAMAM–Gd G7 remained longer in normal blood vessels, it was also penetrated through leaky tumor vessels with an upper limit pore size of 12 nm and produced a poorer contrast in the tumor vasculature compared with PAMAM–Gd G8 (99,102). In addition, PAMAM–Gd G8 also exhibited restricted distribution in lymphatic vessels with a low permeability to surrounding tissues after intracutaneous injection (103,104). One more important factor is the central core molecules which are attributed to the hydrophobicity of dendrimers. DAB–PPI dendrimers (hydrophobic DAB core) revealed a more rapid blood clearance for predominant accumulation which was more than two-fold higher in the liver compared with PAMAM dendrimers of a similar generation and surface functionality (105). As previously mentioned, this might be explained by the opsonization for recognition by RES. Taking these factors into consideration, the dendrimer type and generation critically influence the biodistribution profiles associated with the organ-specific passive targeting of dendrimer–Gd for MRI imaging: for example, PAMAM–Gd G2–4 for the kidney/bladder, PAMAM–Gd G4–7 for normal vasculature, PAMAM–Gd G8 for the tumor vasculature or the lymphatic circulation, and DAB–PPI–Gd for the liver (10) (Fig. 3).

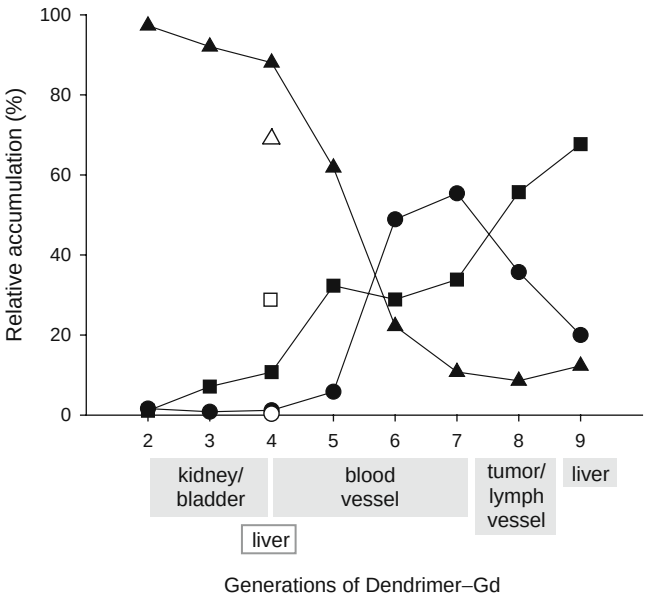

Fig. 3 The relative accumulation of Dendrimer–Gd with different size/ generations for specific organ imaging after intravenous administration in mice. Blood (*black circle*), liver (*black square*), and kidney (*black triangle*) accumulation of PAMAM–Gd with ethylenediamine (filled) and DAB–PPI–Gd (open) dendrimers. (Adapted from (98,99,105,114)).

Surface Modification

Charge

The surface of cationic dendrimers is commonly composed of amine groups exhibiting positive charges in a physiological environment. This is not only associated with potential toxicity (see section on structure-related toxicity) but also nonspecific accumulation after administration. Upon intravenous or intraperitoneal injection, cationic PAMAM dendrimers exhibit a fast clearance from the body with a low blood level (~1% of dose) and high accumulation in the liver, kidney, spleen, lung and pancreas without any specific preference (27,28,106). This is coincident with the rapid blood clearance with low AUC and high hepatic and renal clearance of lysine and ornithine dendrimers in a charge-dependent manner (41) as shown in Fig. 2. However, there was negligible urinary excretion, suggesting tight binding of these amino acid dendrimers in the kidney. Recently, Boyd *et al.* examined the fate of lysine dendrimers and their biodegradability by tracking lysine dendrimers with an interior ^{3}H-lysine branch unit to preserve the positive surface charge (25). The natural (L-form) and unnatural (D-form) lysine were capped at the periphery of the L-lysine G3 dendrimer to obtain L- or -D-lysine G4 dendrimers, respectively. The profile of the L-lysine G4 dendrimer was characterized by an initially rapid fall then an increase to a maximum plateau of the plasma concentration, whereas the D-lysine G4 dendrimer showed only a rapid clearance without redistribution in the blood pool. Unlike the unnatural D-lysine dendrimers, L-lysine dendrimers were expected to undergo proteolytic degradation into free ^{3}H-lysine amino acid. This would support the incorporation of free ^{3}H-lysine for protein biosynthesis resulting in redistribution at the later phase. Accordingly, the high volume of distribution correlated with the rapid blood clearance reflects the rapid binding of cationic lysine dendrimers partly to the vascular endothelium in a process driven by electrostatic interactions (25,107). This nonspecific binding is closely involved in the significantly high uptake via endocytosis with low permeability of cationic PAMAM G4 dendrimers across Caco-2 cells in a generation-dependent fashion (34,108,109).

On the other hand, anionic COOH– (G2.5–5.5) (28) and neutral acetyl (Ac)– (G5) (110) PAMAM dendrimers showed a higher blood circulation (20–40% of dose) with a lower liver accumulation, which was coincident with the EPR effect of anionic PAMAM G3.5 complexed-cisplatin for effective chemotherapy (76). It might not be essential in all cases for prolonged blood retention by anionic manipulation. Recently, Kaminskas *et al.* studied the biodistribution of anionic arylsulfonate or succinate-modified lysine dendrimers G3–4 (95). The anionic arylsulfonate-lysine dendrimers (MW 10–14 kDa) were highly retained in the blood circulation with a five-fold increase in half-life more than succinate-lysine dendrimers (MW 7.4 kDa), which were predominately eliminated by urinary excretion similar to succinate-PAMAM G4 dendrimers (111). As expected, the more anionic charge and greater size of the arylsulfonate-lysine dendrimers, the higher their uptake in the RES, which might be due to the scavenger receptor-mediated process as previously described (89,95). In parallel with the cationic lysine dendrimers, the metabolizable arylsulfonate-lysine dendrimers could be redistributed as a metabolic product and finally excreted into the urine, whereas the non-metabolizable counterpart remained in the liver for 30 h.

The effect of the anionic surface property has been focused on the epithelial permeability in terms of oral drug delivery. Anionic PAMAM dendrimers (G2.5–3.5) displayed a higher serosal transfer rate with a lower uptake in the rat intestine-everted sac system compared with cationic species (108). Unlike that of cationic dendrimers, the increased permeability is correlated with the increased size of the anionic dendrimers (112) and the increased degree of acetylation in cationic dendrimers (34). Kitchens *et al.* extensively studied the permeability of anionic (COOH–), cationic (NH_2–) and neutral (OH–) charged PAMAM across Caco-2 cells examined using FITC-labeled dendrimers and ^{14}C-mannitol as a paracellular transport marker (112). The overall rank order of PAMAM permeability was postulated as G3.5–COOH > G2–NH_2 > G2.5–COOH > G1.5–COOH > G2–OH. The high permeability of charged PAMAM dendrimers (except for G2–NH_2) was presumably caused by the reversible reduction of trans-epithelial electrical resistance (TEER) and disruption of tight junction proteins for opening this channel (112). Kolhatkar *et al.* alternatively demonstrated that the permeability enhancement of fully Ac–PAMAM G4 dendrimers was a function of the reduced hydrophilic repulsion for a more compact structure assembly and suppression of nonspecific cellular binding (34). However, the enhanced paracellular transport by partially and fully Ac–PAMAM G4 dendrimers was not associated linearly with the TEER values, since a modest uptake was also observed. The epithelial transfer mechanism of anionic dendrimers might be dominated by the paracellular route, whereas that of cationic or acetylated dendrimers might involve a combined effect on the paracellular and transcellular pathways (34,108,112).

PEGylation

Despite reduced nonspecific interaction, the neutral dendrimers such as polyester dendrimers (MW 3.8–24 kDa) could not produce a sufficiently long blood circulation, since their small and compact dendritic architecture resulted in rapid renal excretion (43,113). PEGylation

associated with increased hydrophilicity and reduced opsonization (90) is commonly used to overcome this problem through the EPR effect, which has been widely used for passive tumor targeting (3). Margerum *et al.* first reported the PEGylation of PAMAM–Gd G2–3 for predicting biodistribution (106). After intravenous injection, PEG–PAMAM–Gd with PEG-2 and -5 kDa (MW 20–69 kDa) showed a 15–110-fold increased blood half-life (2.8–20 h) compared with the parent species. Correspondingly, PAMAM–Gd G4 dendrimers with 1 or 2 molecules of PEG-20 kDa (MW 77–97 kDa) had a modest effect with only a 2–3-fold increased blood half-life (2.5 h) with 10–20% of the blood level, dramatically reduced renal accumulation, and increased urinary and fecal excretions (114). Hashida and colleagues showed the almost 20-fold increased blood retention time for 20–40% of the blood level over 24 h when lysine G6 dendrimers were modified with 60% surface functionality of PEG-5 kDa (MW 400 kDa) (41). These dendrimers exhibited a high AUC and low hepatic and renal clearance at 24 h post-injection (Fig. 2). Accordingly, the increased blood half-life with the EPR effect of PEGylated dendrimer-doxorubicin with PEG-5 kDa (MW 40–115 kDa) induced the tumor accumulation of doxorubicin for effective anticancer activity in tumor-bearing mice (58,115). In addition, the increased generations of PEGylated lysine (G3 to G4) with PEG-2 kDa (MW 34 to 68 kDa) (116) and PEGylated bow-tie dendrimers (G1 to G3) with PEG-10 kDa (MW 22 to 85 kDa) (38) prolonged blood retention time from 24 to 75 and 8 to 40 h, respectively. However, this enhanced effect of dendrimer generation was less pronounced in PEGylated lysine dendrimers with PEG-0.2 kDa (MW 6–11 kDa) (116).

Although the PEG effect in these studies shows the same trend for increased blood retention, the disparity in the degree of enhancement illustrates the significant role of the number and molecular mass of PEG which govern the total MW and architecture flexibility of PEGylated dendrimers. As expected, at least a two-fold increased elimination half-life and decreased localization in the liver and kidney were observed with the 60% PEGylation (PEG-5 kDa) of lysine G6 dendrimers (MW 400 kDa) (46) and 100% PEGylation (PEG-0.57 kDa) of lysine G4 dendrimers (MW 22 kDa) (117) compared with the 8% (MW 66 kDa) and 50% (MW 13 kDa) PEGylation counterparts, respectively. Albeit sufficient shielding of the nonspecific binding in the liver, partially (50%) PEG–lysine G4 dendrimers with PEG-0.57 kDa were not able to resist kidney accumulation, even with additional surface modification with 50% acetylation (117) or methotrexate conjugation (55). This was explained by their total MW being lower than 30–50 kDa for glomerular filtration compared with their fully PEGylated counterparts. Kaminskas *et al.* studied a series of fullly and partially PEGylated lysine dendrimers with different PEG molecular mass on the changes in biodistribution profiles (55,117). The blood half-life of PEGylated lysine G4 dendrimers (MW 11–68 kDa) increased from 0.7 h to 75.4 h when the PEG mass increased from 0.2 to 2 kDa. On the other hand, the renal clearance was almost completely abolished while the non-renal clearance was predominant. This phenomenon was more pronounced with higher generations of lysine dendrimers. The increased generations and PEG molecular mass resulting in the greater total MW of PEGylated dendrimers strongly affects the length of blood retention, reduction in liver accumulation and renal clearance (55,117). These emphasize the impact of the total MW of PEGylated dendrimers controlled by not only the degree of PEGylation but also the molecular mass of PEG for alteration of biodistribution and excretion. Nevertheless, these might not be the only factors, since Gillies *et al.* reported the effect of PEG and architecture flexibility of bow-tie polyester dendrimers on pharmacokinetic behavior (38,118). Asymmetrically PEGylated bow-tie polyester dendrimers G2–3 with PEG-5, -10 or -20 kDa on one side of the dendron (MW > 40 kDa) showed similar results to those discussed above. Interestingly, the higher total MW of bow-tie G2 with four molecules of PEG-10 kDa (MW 34.9 kDa) had a nine-fold higher urinary excretion compared with the lower total MW of G3 with eight molecules of PEG-5 kDa (MW 28.3 kDa). This suggests that the more flexible lower branched dendrimers are more easily deformed and pass through the glomerular pores, resulting in a higher urinary excretion despite the slightly higher MW (15), which correlates to the phenomenon of linear or loosely coiled polymers (101,119). More interestingly, PEGylated bow-tie G3 dendrimers with a total MW ~160 kDa ($t_{1/2}$ = 50 h) had a significantly lower half-life compared with PEGylated lysine dendrimers with a total MW of 68 kDa ($t_{1/2}$ = 75 h), suggesting that the potentially higher clearance was due to the greater flexibility of the bow-tie polyester dendrimers (38,116). Recently, Lim *et al.* directly compared the PEG effect in symmetrical PEG-modified polytriazine dendrimers to asymmetrical PEG-modified bow-tie polyester dendrimers (120). Based on the total MW and flexibility assumption, asymmetrically PEG-modified bow-tie dendrimers seem to require a longer PEG of 10–20 kDa (MW 85–160 kDa) to obtain a similar half-life of 40–50 h as symmetrically PEG-modified dendrimers with a shorter PEG of 2 kDa (MW 30–70 kDa). The relationship between the blood half-life and PEG is summarized in Fig. 4.

Targeting Ligand

A number of studies involving the active targeting approach have examined in tumor chemotherapy and diagnosis using antibody, folic acid, avidin-biotin complex, RGD peptide,

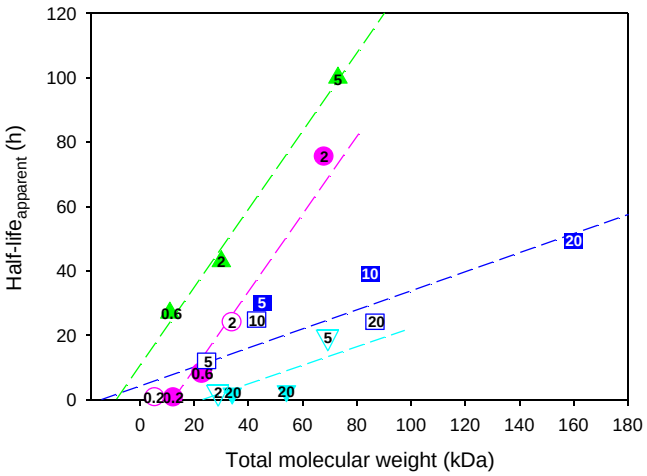

Fig. 4 The effect of the total molecular weight of PEGylated dendrimers on their apparent half-life. Symmetrical PEG-modification of dendrimers; PEG–PAMAM dendrimers G3 (*white down-pointing triangle*) and G4 (*black down-pointing triangle*); PEG–lysine dendrimers G3 (*white circle*) and G4 (*black circle*); PEG–polytriazine dendrimers G2 (*black triangle*). Asymmetrical PEG-modification of dendrimers: PEG–bow-tie polyester dendrimers dendrimers G2 (*white square*) and G3 (*black square*). The numbers inserted in symbols indicate the molecular mass of the PEG chains. (Adapted from (106,114,116,118,120)).

and carbohydrate molecules. These targeting ligands are recognized by the corresponding receptors which are highly expressed on the tumor cells compared with restricted expression in normal cells. It is widely known that the ligand-receptor interaction is critically dependent on the binding affinity and ligand density for targeting molecules (121–123). Taking this into consideration, the multivalency of conjugated ligands on dendrimers can improve tumor targeting. Therefore, highly tumor-targeted dendrimers would alter the biodistribution profiles, and their efficiency could be evaluated as a ratio of the amount at the target (tumor) to the non-target site in parallel with the therapeutic availability (TA) as described above.

The antibody-dendrimer targeting molecules were extensively studied by Barth, Yang *et al.* Anti-EGF antibody was conjugated with boronated PAMAM G4 dendrimers for targeting to EGF receptor-expressing tumor cells, including solid B16 melanoma (124) and intracerebral implanted EGFR-transfected C6 (50) and F98 glioma (125) models, in boron neutron capture therapy (BNCT). At 24 h post-intratumoral injection, boronated PAMAM-EGF conjugates were highly localized (22–33% of dose/g) in EGFR-positive glioma with a tumor/blood ratio of 16 compared with the amount in wild-type glioma (5–9% of dose/g) or non-targeted PAMAM dendrimers in EGFR-positive cells (0.3% of dose/g) (50). Accordingly, the high tumor/brain ratios (3.5–16 in range) of PAMAM–EGF conjugates indicated the efficient targeting to EGFR-positive tumors. The greater EGFR specificity of cetuximab and L8A4 antibodies showed the increased accumulation in EGFR-positive glioma by 1.5–2-fold for antibody–PAMAM or combined antibody–PAMAM conjugates, respectively (63,64,126). These led to the improved accumulation of methotrexate or boron molecules delivered by EGF antibody–PAMAM conjugates with a high target/non-target ratio for prolonged survival in EGF-positive glioma-bearing mice (63).

Folic acid, a small targeting molecule, has been extensively used with folate-binding proteins on tumor cells, including ovarian and oral-epidermal carcinoma, because of their small size, easy handling for chemical conjugation, high stability and low cost (9,36). Folate-modified PAMAM dendrimers showed significantly high accumulation (6–9% of dose/g) with a tumor/blood ratio of 35 in folate-overexpressing human KB tumors in immunodeficient mice over four days after intraperitoneal (48) and intravenous administrations (36). However, the tumor accumulation, as much as 2% of the dose/g, was comparable with the blood level in case of unmodified PAMAM dendrimers (48,127). This suggested a selective accumulation of folate-modified PAMAM only in folate-positive rather than folate-negative tumors (127). However, the low hepatic and renal localization was also observed due to the presence of folate receptors in hepatic macrophages and renal proximal tubules (36,48,49,127). Corresponding to the pharmacokinetic behavior of folate–PAMAM dendrimers, folate–PAMAM–methotrexate conjugates elicited as much as ten-fold higher suppression of tumor growth compared with free methotrexate at an equivalent dose (36).

Another targeting molecule is the avidin-biotin complex system, since it has been shown to be taken up extensively by tumor and liver cells (128). Wilbur *et al.* showed that ^{125}I-labeled iodobenzoate-biotinylated PAMAM dendrimers (G0–4) were quickly cleared, giving low blood levels and high kidney and liver accumulation compared with their unmodified counterparts (129). The use of the avidin-biotin system has been extended for MRI, Gd-neutron capture therapy and gene delivery in a collaboration between the Kobayashi, Brechbiel and Konishi groups (130,131). After intraperitoneal administration, avidin-modified PAMAM–Gd G6 conjugates exhibited specific accumulation in intraperitoneally disseminated SHIN3 ovarian cancer cells (103% of dose/g) with 366- and 3.4-fold greater values than Gd–DTPA (0.28% of dose/g) and unmodified PAMAM–Gd (30% of dose/g), respectively (130). The tumor/normal tissue ratio was greater than 17 at 6 h and increased to 638 at 24 h post-dosing. Interestingly, this system could be applied for activated clearance of biotin–PAMAM–Gd from the body using an avidin chase (131). The concept of an avidin chase is based on the binding of avidin to biotin macromolecules for subsequent high accumulation

in the liver via avidin recognition. The circulating biotin–PAMAM–Gd in the blood pool was cleared within 2 min following injection of avidin after 4 min. This mechanism might not affect the formerly vascular leaked molecules. Therefore, the imaging of vascular leakage could be improved.

Other targeting molecules, such as cyclic RGD peptide (132,133), mannose (52), and transferrin (134), have been conjugated with dendrimers and exhibited effective targeting. The use of ligands that can be recognized by normal or non-target tissue, such as folate or avidin, can produces less targeting efficiency, which may potentially influence therapeutic outcomes and side effects. It is noteworthy that the types of receptors which are restricted expressed only on the target cells, and the receptor binding affinity for tuning disposition is exhibited only in the target cells.

Routes of Administration

The anatomy and physiology are barriers for accessibility of drug molecules to the target site which crucially depends on the route of administration. In this regard, the same dendrimers administered by different routes could show different biodistribution and pharmacokinetic profiles resulting in altered therapeutic efficacy and side effects. As there is ready access to the systemic circulation by intravenous administration, the rapid and high exposure to most organs induces nonspecific interactions and excretion, although active targeting is used. Lower exposure, especially to the RES, seems to reduce the potential for accumulation in non-target tissues. According to this assumption, Malik *et al.* demonstrated a two-fold increased blood level (35–40% of dose) with reduced hepatic accumulation of anionic PAMAM dendrimers after intraperitoneal administration compared with systemic administration via the tail vein (15–20% of dose) (28). In order to design hepatic targeting vectors for oligonucleotides, the avidin-biotin system was selected (135). Although avidin-oligonucleotide complex resulted in high hepatic targeting, the avidin–PAMAM/oligonucleotide complex did not successfully target the liver (only 20% of dose/g) because a large amount was trapped in the lungs (125–180% of dose/g). This was probably due to the positive charge and large complex size corresponding to the PAMAM G9/plasmid DNA complex (136). However, the intraperitoneally injected avidin–PAMAM/oligonucleotide complex exhibited high tumor accumulation in peritoneal disseminated SHIN3 tumor-bearing mice because of the direct target accessibility (137), although only moderately high hepatic uptake was observed (130).

Local administration directly to the target site is used for improved biodistribution and pharmacokinetics resulting in effective delivery and therapeutic efficacy. A key example is the brain delivery system, since the blood-brain barrier hinders drug penetration to the brain. After intravenous administration, the delivery of dendrimer-based drugs to the brain was significantly improved using transferrin (134) or EGF antibody (50) as targeting ligands. However, only 0.07 or 0.01% of dose/g was observed in the transferrin receptor-expressing brain tissue or EGF-positive glioma cells, respectively. As for boronated PAMAM–EGF conjugates, a high accumulation (5–20% of dose/g) was observed in the liver and spleen, where there was a response by the EGF receptors present (138) or the inherent propensity of the dendrimers (105). The accumulation in these non-target organs was negligible (less than 0.2% of dose/g) after intracerebral or intratumoral administrations (50). More pronounced targeting of PAMAM–EGF conjugates was observed by intracerebral injection with pressure called "convection enhanced delivery" (63,139). The pressure gradient induces the homogenous distribution of PAMAM–EGF conjugates to large regions of the brain resulting in a larger volume of distribution (7.2-fold increase) and two-fold higher accumulation in the EGF-positive glioma compared with conventional intracerebral injection (63,64,126,139). Other local administration routes, including intratracheal or pulmonary administration (140), and transdermal delivery (77,141) of dendrimer-based drugs, have been demonstrated. Similar findings were obtained for the increased localization of dendrimer-based drugs at the target site and prevented RES uptake via the hepatic first-pass effect for improved bioavailability and the avoidance of side effects in agreement with previous studies of liposomal drugs given by intratracheal administration (142,143).

The role of subcutaneous administration of dendrimers has been studied for lymphatic distribution after absorption to peripheral and central lymphatic system, and systemic distribution by blood absorption pathway (144). This could lead to a 50-fold increased tumor accumulation of subcutaneously injected anionic PAMAM–cisplatin for enhanced anticancer activity in B16F10 tumor-bearing mice compared with intravenous injection (76). Kaminskas *et al.* demonstrated the increased lymphatic accumulation of PEGylated lysine dendrimers of different sizes (145). Although the lymphatic disposition of dendrimers was closely related to the function of PEG and the dendritic size, injection by the subcutaneous route only slightly prolonged the plasma half-life (1.5–2-fold increase) and gradually increased the lymphatic accumulation with a two-fold higher bioavailability (29%) of PEGylated-lysine dendrimers (PEG-0.57 kDa) in a lymph-cannulated rat model. However, the clear effect obtained by different routes was meaningless in lysine dendrimers modified with larger PEG, since the redistribution between the blood and lymphatic circulation occurred after a prolonged circulation half-life (104,145).

Oral delivery is the major route for clinical use and by far the most convenient with good patient compliance. However, the main problems include low bioavailability involving poor water solubility, low penetration across intestinal membranes (absorption into blood circulation) and side effects. Dendrimers have been used as absorption enhancers as well as drug vehicles (146). It seems that the biodistribution of orally administered dendrimers might spread out along the gastrointestinal tract, leading to very low drug concentrations after systemic absorption. Florence and colleagues demonstrated that alkylated (C_{12}) lysine G4 dendrimer (MW 6.3 kDa) was extensively recovered in the small intestine (5–17% of dose), especially Peyer's patches, whereas only 1–3% was found in the blood and less than 1% in the liver, spleen and kidney over 24 h (147). In addition, Ke *et al.* demonstrated the enhanced bioavailability of doxorubicin complexed with PAMAM G3 dendrimers after oral administration (148). The plasma profile of doxorubicin in PAMAM dendrimers was characterized by a rapid increase after 1 h (14 μM) with later gradual decrease (5 μM) over 24 h providing a 300-fold increase of AUC compared with the very low systemic absorption of free doxorubicin (less than 1 μM). Although orally administered dendrimer-based drugs showed better bioavailability than free drugs, it was much lower drug concentration in the blood circulation compared to intravenous administration. The oral delivery of dendrimer-based drugs encounters many tasks and needs further investigation and development.

Although systemic administration provides rapid distribution to target and non-target organs, local administration would be superior for desired biodistribution with higher bioavailability and pharmacokinetics, especially in the case of drugs with poor access to the target site.

PERSPECTIVE FOR CLINICAL TRANSLATION

Although the number of publications on dendrimer research has gradually increased over the past two decades, only a few dendrimers are undergoing clinical trials compared with other nanoparticles such as liposomes (149). The dendrimer–Gd conjugate, Gadomer-17, was first clinically used as an MRI imaging agent by Schering (150). The pharmaceutical application of dendrimers has recently undergone the clinical translation since the first dendrimer called Vivagel® has been translated from research studies to clinical trials as a new FDA drug application (151). Vivagel®, developed by Starpharma (Melbourne, Australia), is a formulation of polyanionic lysine G4 dendrimers with an anionic surface of naphthalene-disulfonate (SPL7013) in a Carbopol® gel. It exhibits antiviral activity against HIV and HSV for the treatment of sexually transmitted infections and is given by intravaginal administration (152). Complete preclinical and phase I clinical studies have shown that 0.5–3% SPL7013 formulations are safe and well tolerated after seven-day vaginal application without systemic absorption (151–153). A phase II clinical trial of Vivagel® is ongoing with fast track status. Another dendrimer undergoing preclinical study is the multiantigenic peptide PHSCN-lysine dendrimer for inhibition of invasion and growth of breast cancer cells via α5β1 integrin-selective recognition in a metastatic murine cancer model (154).

In 2006, the FDA launched a Nanotechnology Task Force for critical regulatory issues regarding nanomaterials containing drug products. Since they contain FDA-approved drugs, nanoparticle formulations are classified as a new formulation with required submission of an Investigational New Drug Application (IND), not a New Molecular Entity (NME) (149). Accordingly, guidelines for IND are being developed to address specific issues of nanomaterials containing drug products which have unique or physicochemical properties distinct from drug molecules. This highlights the importance of biodistribution and pharmacokinetics as a topic of the Absorption, Distribution, Metabolism and Excretion (ADME) assessment. The FDA requires biodistribution and pharmacokinetic studies of each component of nanomaterials containing drugs compared with free drugs. In the case of dendrimer-based drugs, this means that the studies of dendrimer, free drug, and dendrimer-drug assembly are needed which could be conducted using dual-labeled pharmacokinetics in each species. The impact of dendrimer physicochemical properties on biodistribution behavior has been clearly emphasized in this review. Although it could contribute to generalizations regarding various concerns, the disparity of data from various sources and experimental methods leads to a slightly different conclusion. One of most important factors is the labeling methods, which could trigger a change in dendrimer surface properties, dendrimer-disattachment of unstable probes (110,155), redistribution of probe after metabolism (25,83,156), or receptor recognition of labeling probe (43). These may affect the alteration of pharmacokinetic profiles. In addition, the FDA recommends a long-term study as a standard guideline to assess the safety and efficacy. As reported in the literature, dendrimers such as PAMAM are well-tolerated in mice without any serious toxicity over time (42,43). However, some vacuolization of the cytoplasm in the liver was observed after long-term administration of cationic PAMAM dendrimers G3–7 at 2.5–10 mg/kg (27). It is important to consider not only the properties of the dendrimer or dendrimer-based drug but also the experimental design for careful evaluation and interpretation of pharmacokinetic and biodistribution studies with regard to safety and efficacy during clinical use.

CONCLUSION

The unique dendritic structure of dendrimers consisting of a central core, internal cavity and surface functions makes dendrimers an ideal vector for drug or imaging molecules for therapeutic or diagnostic purposes. Dendrimer-based drugs can be prepared by chemical conjugation, physical encapsulation or complexation. The controllable properties of dendrimers, including size, charge, and chemical modification, provide an excellent platform for passive and active targeting. These properties dramatically affect the biodistribution and pharmacokinetic characteristics influencing safety and efficacy of dendrimers. By using a size of more than 30–50 kDa with a slight anionic surface charge or PEGylation, dendrimers can be obtained with low cytotoxicity and prolong the blood retention with less nonspecific binding after intravenous administration. The pharmacokinetics can be further improved using ligand-modified dendrimers which can be recognized by the corresponding receptors restricted only at the target tissue to increase accumulation for effective therapy. Finally, the appropriate route of administration will provide the desired pharmacokinetic parameters, especially better accessibility to the target site. The distinct biodistribution and pharmacokinetics influenced by dendrimer properties suggest their function as organ-specific applications for particular purposes. This review hopefully gives some useful information on pharmacokinetic considerations for the rationale design of dendrimers for the controlled delivery of drugs and imaging reagents for therapeutic or diagnostic applications.

ACKNOWLEDGMENTS

We wish to express sincere thanks to Dr. Yasuhiko Hashida of the iCeMS, Kyoto University, Kyoto, Japan for graphic assistance in Fig. 1a. We are grateful for financial support from W. Wijagkanalan by the Japan Society for the Promotion of Sciences (JSPS) through a JSPS research fellowship for young scientists.

REFERENCES

1. Duncan R. The dawning era of polymer therapeutics. Nat Rev Drug Discov. 2003;2:347–60.
2. Matsumura Y, Kataoka K. Preclinical and clinical studies of anticancer agent-incorporating polymer micelles. Cancer Sci. 2009;100:572–9.
3. Matsumura Y, Maeda H. A new concept for macromolecular therapeutics in cancer chemotherapy: mechanism of tumoritropic accumulation of proteins and the antitumor agent smancs. Cancer Res. 1986;46:6387–92.
4. Buhleier E, Wehner W, Vogtle F. "Cascade"-and "Nonskid-Chain-like" syntheses of molecular cavity topologies. Synthesis. 1978;155.
5. Denkewalter RG, Kolc J, Lukasavage WJ. Macromolecular highly branched homogeneous compound based on lysine units. 1981.
6. Tomalia DA, Baker H, Dewald J, Hall M, Kallos G, Martin S, *et al.* A new class of polymer: starburst-dendritic macromolecules. Polym J. 1985;17:117–32.
7. Newkome GR, Yao Z, Baker GR, Gupta VK. Micelles. Part 1. Cascade molecules: a new approach to micelles. A[27]-arbosol. J Org Chem. 1985;50:2003–4.
8. Svenson S, Tomalia D. Dendrimers in biomedical applications–reflections on the field. Adv Drug Deliv Rev. 2005;57:2106–29.
9. Wolinsky J, Grinstaff M. Therapeutic and diagnostic applications of dendrimers for cancer treatment. Adv Drug Deliv Rev. 2008;60:1037–55.
10. Kobayashi H, Brechbiel M. Nano-sized MRI contrast agents with dendrimer cores. Adv Drug Deliv Rev. 2005;57:2271–86.
11. Sugao Y, Watanabe K, Higuchi Y, Kurihara R, Kawakami S, Hashida M, *et al.* NFkappaB decoy delivery using dendritic poly (l-lysine) for treatment of endotoxin-induced hepatitis in mice. Bioorg Med Chem. 2009;17:4990–5.
12. Dufès C, Uchegbu I, Schätzlein A. Dendrimers in gene delivery. Adv Drug Deliv Rev. 2005;57:2177–202.
13. Hawker C, Fréchet J. Preparation of polymers with controlled molecular architecture. A new convergent approach to dendritic macromolecules. J Am Chem Soc. 1990;112:7638–47.
14. Fréchet J, Hawker C, Gitsov I, Leon JW. Dendrimers and hyperbranched polymers: two families of three-dimensional macromolecules with similar but clearly distinct properties. J Macromol Sci Pure Appl Chem. 1996;33:1399–425.
15. Lee C, MacKay J, Fréchet J, Szoka F. Designing dendrimers for biological applications. Nat Biotechnol. 2005;23:1517–26.
16. Duncan R, Izzo L. Dendrimer biocompatibility and toxicity. Adv Drug Deliv Rev. 2005;57:2215–37.
17. Cheng Y, Xu T. The effect of dendrimers on the pharmacodynamic and pharmacokinetic behaviors of non-covalently or covalently attached drugs. Eur J Med Chem. 2008;43:2291–7.
18. Menjoge A, Kannan R, Tomalia D. Dendrimer-based drug and imaging conjugates: design considerations for nanomedical applications. Drug Discov Today. 2010;15:171–85.
19. de Brabander-van den Berg E, Meijer E. Poly(propylene imine) dendrimers: large-scale synthesis by heterogeneously catalyzed hydrogenations. Angew Chem Int Ed Engl. 1993;32:1308–11.
20. Spetzler J, Tam J. Unprotected peptides as building blocks for branched peptides and peptide dendrimers. Int J Pept Protein Res. 1995;45:78–85.
21. Fréchet J. Functional polymers and dendrimers: reactivity, molecular architecture, and interfacial energy. Science. 1994;263:1710–5.
22. Zhang W, Simanek E. Dendrimers based on melamine. Divergent and orthogonal, convergent syntheses of a G3 dendrimer. Org Lett. 2000;2:843–5.
23. Wu P, Feldman A, Nugent A, Hawker C, Scheel A, Voit B, *et al.* Efficiency and fidelity in a click-chemistry route to triazole dendrimers by the copper(i)-catalyzed ligation of azides and alkynes. Angew Chem Int Ed Engl. 2004;43:3928–32.
24. McGrath D. Dendrimer disassembly as a new paradigm for the application of dendritic structures. Mol Pharm. 2005;2:253–63.
25. Boyd B, Kaminskas L, Karellas P, Krippner G, Lessene R, Porter C. Cationic poly-L-lysine dendrimers: pharmacokinetics, biodistribution, and evidence for metabolism and bioresorption after intravenous administration to rats. Mol Pharm. 2006;3:614–27.
26. Vega-Villa K, Takemoto J, Yáñez J, Remsberg C, Forrest M, Davies N. Clinical toxicities of nanocarrier systems. Adv Drug Deliv Rev. 2008;60:929–38.
27. Roberts J, Bhalgat M, Zera R. Preliminary biological evaluation of polyamidoamine (PAMAM) Starburst dendrimers. J Biomed Mater Res. 1996;30:53–65.

28. Malik N, Wiwattanapatapee R, Klopsch R, Lorenz K, Frey H, Weener J, *et al.* Dendrimers: relationship between structure and biocompatibility *in vitro*, and preliminary studies on the biodistribution of 125I-labelled polyamidoamine dendrimers *in vivo*. J Control Release. 2000;65:133–48.
29. Ohsaki M, Okuda T, Wada A, Hirayama T, Niidome T, Aoyagi H. *In vitro* gene transfection using dendritic poly(L-lysine). Bioconjug Chem. 2002;13:510–7.
30. Hong S, Bielinska A, Mecke A, Keszler B, Beals J, Shi X, *et al.* Interaction of poly(amidoamine) dendrimers with supported lipid bilayers and cells: hole formation and the relation to transport. Bioconjug Chem. 2004;15:774–82.
31. Jevprasesphant R, Penny J, Jalal R, Attwood D, McKeown N, D'Emanuele A. The influence of surface modification on the cytotoxicity of PAMAM dendrimers. Int J Pharm. 2003;252:263–6.
32. Yang H, Lopina S, DiPersio L, Schmidt S. Stealth dendrimers for drug delivery: correlation between PEGylation, cytocompatibility, and drug payload. J Mater Sci Mater Med. 2008;19:1991–7.
33. Bhadra D, Bhadra S, Jain S, Jain N. A PEGylated dendritic nanoparticulate carrier of fluorouracil. Int J Pharm. 2003;257:111–24.
34. Kolhatkar R, Kitchens K, Swaan P, Ghandehari H. Surface acetylation of polyamidoamine (PAMAM) dendrimers decreases cytotoxicity while maintaining membrane permeability. Bioconjug Chem. 2007;18:2054–60.
35. Asthana A, Chauhan A, Diwan P, Jain N. Poly(amidoamine) (PAMAM) dendritic nanostructures for controlled site-specific delivery of acidic anti-inflammatory active ingredient. AAPS PharmSciTech. 2005;6:E536–42.
36. Kukowska-Latallo J, Candido K, Cao Z, Nigavekar S, Majoros I, Thomas T, *et al.* Nanoparticle targeting of anticancer drug improves therapeutic response in animal model of human epithelial cancer. Cancer Res. 2005;65:5317–24.
37. Lee C, Yoshida M, Fréchet J, Dy E, Szoka F. *In vitro* and *in vivo* evaluation of hydrophilic dendronized linear polymers. Bioconjug Chem. 2005;16:535–41.
38. Gillies E, Dy E, Fréchet J, Szoka F. Biological evaluation of polyester dendrimer: poly(ethylene oxide) "bow-tie" hybrids with tunable molecular weight and architecture. Mol Pharm. 2005;2:129–38.
39. Miyano T, Wijagkanalan W, Kawakami S, Yamashita F, Hashida M. Anionic amino acid dendrimer-trastuzumab conjugates for specific internalization in HER2-positive cancer cells. Mol Pharm. 2010;7:1318–27.
40. Neerman M, Zhang W, Parrish A, Simanek E. *In vitro* and *in vivo* evaluation of a melamine dendrimer as a vehicle for drug delivery. Int J Pharm. 2004;281:129–32.
41. Okuda T, Kawakami S, Maeie T, Niidome T, Yamashita F, Hashida M. Biodistribution characteristics of amino acid dendrimers and their PEGylated derivatives after intravenous administration. J Control Release. 2006;114:69–77.
42. Chen H, Neerman M, Parrish A, Simanek E. Cytotoxicity, hemolysis, and acute *in vivo* toxicity of dendrimers based on melamine, candidate vehicles for drug delivery. J Am Chem Soc. 2004;126:10044–8.
43. Padilla De Jesús O, Ihre H, Gagne L, Fréchet J, Szoka FJ. Polyester dendritic systems for drug delivery applications: *in vitro* and *in vivo* evaluation. Bioconjug Chem. 2002;13:453–61.
44. Tomalia DA, Naylor AM, Goddard III WA. Starburst dendrimers: molecular-level control of size, shape, surface chemistry, topology, and flexibility from atoms to macroscopic matter. Angew Chem Int Ed Engl. 1990;29:138–75.
45. Kojima C, Kono K, Maruyama K, Takagishi T. Synthesis of polyamidoamine dendrimers having poly(ethylene glycol) grafts and their ability to encapsulate anticancer drugs. Bioconjug Chem. 2000;11:910–7.
46. Okuda T, Kawakami S, Akimoto N, Niidome T, Yamashita F, Hashida M. PEGylated lysine dendrimers for tumor-selective targeting after intravenous injection in tumor-bearing mice. J Control Release. 2006;116:330–6.
47. Gajbhiye V, Kumar PV, Tekade RK, Jain NK. Pharmaceutical and biomedical potential of PEGylated dendrimers. Curr Pharm Des. 2007;13:415–29.
48. Shukla S, Wu G, Chatterjee M, Yang W, Sekido M, Diop L, *et al.* Synthesis and biological evaluation of folate receptor-targeted boronated PAMAM dendrimers as potential agents for neutron capture therapy. Bioconjug Chem. 2003;14:158–67.
49. Chandrasekar D, Sistla R, Ahmad F, Khar R, Diwan P. The development of folate-PAMAM dendrimer conjugates for targeted delivery of anti-arthritic drugs and their pharmacokinetics and biodistribution in arthritic rats. Biomaterials. 2007;28:504–12.
50. Yang W, Barth R, Adams D, Soloway A. Intratumoral delivery of boronated epidermal growth factor for neutron capture therapy of brain tumors. Cancer Res. 1997;57:4333–9.
51. Shukla R, Thomas T, Peters J, Desai A, Kukowska-Latallo J, Patri A, *et al.* HER2 specific tumor targeting with dendrimer conjugated anti-HER2 mAb. Bioconjug Chem. 2006;17:1109–15.
52. Agashe H, Babbar A, Jain S, Sharma R, Mishra A, Asthana A, *et al.* Investigations on biodistribution of technetium-99m-labeled carbohydrate-coated poly(propylene imine) dendrimers. Nanomedicine. 2007;3:120–7.
53. Gurdag S, Khandare J, Stapels S, Matherly L, Kannan R. Activity of dendrimer-methotrexate conjugates on methotrexate-sensitive and -resistant cell lines. Bioconjug Chem. 2006;17:275–83.
54. Shukla R, Thomas TP, Desai AM, A. K, Park SJ, Baker JR Jr. HER2 specific delivery of methotrexate by dendrimer conjugated anti-HER2 mAb. Nanotechnology. 2008;19:art. no. 295102.
55. Kaminskas L, Kelly B, McLeod V, Boyd B, Krippner G, Williams E, *et al.* Pharmacokinetics and tumor disposition of PEGylated, methotrexate conjugated poly-l-lysine dendrimers. Mol Pharm. 2009;6:1190–204.
56. Lee C, Gillies E, Fox M, Guillaudeu S, Fréchet J, Dy E, *et al.* A single dose of doxorubicin-functionalized bow-tie dendrimer cures mice bearing C-26 colon carcinomas. Proc Natl Acad Sci USA. 2006;103:16649–54.
57. Guillaudeu S, Fox M, Haidar Y, Dy E, Szoka F, Fréchet J. PEGylated dendrimers with core functionality for biological applications. Bioconjug Chem. 2008;19:461–9.
58. van der Poll D, Kieler-Ferguson H, Floyd W, Guillaudeu S, Jerger K, Szoka F, *et al.* Design, synthesis, and biological evaluation of a robust, biodegradable dendrimer. Bioconjug Chem. 2010;21:764–73.
59. Zhu S, Hong M, Zhang L, Tang G, Jiang Y, Pei Y. PEGylated PAMAM dendrimer-doxorubicin conjugates: *in vitro* evaluation and *in vivo* tumor accumulation. Pharm Res. 2010;27(1):161–74.
60. Fox M, Guillaudeu S, Fréchet J, Jerger K, Macaraeg N, Szoka F. Synthesis and *in vivo* antitumor efficacy of PEGylated poly(l-lysine) dendrimer-camptothecin conjugates. Mol Pharm. 2009;6:1562–72.
61. Wiener E, Brechbiel M, Brothers H, Magin R, Gansow O, Tomalia D, *et al.* Dendrimer-based metal chelates: a new class of magnetic resonance imaging contrast agents. Magn Reson Med. 1994;31:1–8.
62. Konda S, Aref M, Brechbiel M, Wiener E. Development of a tumor-targeting MR contrast agent using the high-affinity folate receptor: work in progress. Invest Radiol. 2000;35:50–7.
63. Wu G, Barth R, Yang W, Kawabata S, Zhang L, Green-Church K. Targeted delivery of methotrexate to epidermal growth factor receptor-positive brain tumors by means of cetuximab (IMC-C225) dendrimer bioconjugates. Mol Cancer Ther. 2006;5:52–9.
64. Yang W, Wu G, Barth R, Swindall M, Bandyopadhyaya A, Tjarks W, *et al.* Molecular targeting and treatment of composite EGFR

and EGFRvIII-positive gliomas using boronated monoclonal antibodies. Clin Cancer Res. 2008;14:883–91.
65. Perumal O, Inapagolla R, Kannan S, Kannan R. The effect of surface functionality on cellular trafficking of dendrimers. Biomaterials. 2008;29:3469–76.
66. Najlah M, Freeman S, Attwood D, D'Emanuele A. Synthesis, characterization and stability of dendrimer prodrugs. Int J Pharm. 2006;308:175–82.
67. Kurtoglu Y, Navath R, Wang B, Kannan S, Romero R, Kannan R. Poly(amidoamine) dendrimer-drug conjugates with disulfide linkages for intracellular drug delivery. Biomaterials. 2009;30:2112–21.
68. Jansen J, de Brabander-van den Berg E, Meijer E. Encapsulation of guest molecules into a dendritic box. Science. 1994;266:1226–9.
69. Gupta U, Agashe H, Asthana A, Jain N. Dendrimers: novel polymeric nanoarchitectures for solubility enhancement. Biomacromolecules. 2006;7:649–58.
70. Cheng Y, Li Y, Wu Q, Zhang J, Xu T. Generation-dependent encapsulation/electrostatic attachment of phenobarbital molecules by poly(amidoamine) dendrimers: evidence from 2D-NOESY investigations. Eur J Med Chem. 2009;44:2219–23.
71. Ooya T, Lee J, Park K. Effects of ethylene glycol-based graft, star-shaped, and dendritic polymers on solubilization and controlled release of paclitaxel. J Control Release. 2003;93:121–7.
72. Dhanikula R, Hildgen P. Influence of molecular architecture of polyether-co-polyester dendrimers on the encapsulation and release of methotrexate. Biomaterials. 2007;28:3140–52.
73. Yang H, Morris J, Lopina S. Polyethylene glycol-polyamidoamine dendritic micelle as solubility enhancer and the effect of the length of polyethylene glycol arms on the solubility of pyrene in water. J Colloid Interface Sci. 2004;273:148–54.
74. Dutta T, Jain N. Targeting potential and anti-HIV activity of lamivudine loaded mannosylated poly (propyleneimine) dendrimer. Biochim Biophys Acta. 2007;1770:681–6.
75. Morgan M, Nakanishi Y, Kroll D, Griset A, Carnahan M, Wathier M, *et al.* Dendrimer-encapsulated camptothecins: increased solubility, cellular uptake, and cellular retention affords enhanced anticancer activity *in vitro*. Cancer Res. 2006;66:11913–21.
76. Malik N, Evagorou E, Duncan R. Dendrimer-platinate: a novel approach to cancer chemotherapy. Anticancer Drugs. 1999;10:767–76.
77. Chauhan A, Sridevi S, Chalasani K, Jain A, Jain S, Jain N, *et al.* Dendrimer-mediated transdermal delivery: enhanced bioavailability of indomethacin. J Control Release. 2003;90:335–43.
78. Patri A, Kukowska-Latallo J, Baker JJ. Targeted drug delivery with dendrimers: comparison of the release kinetics of covalently conjugated drug and non-covalent drug inclusion complex. Adv Drug Deliv Rev. 2005;57:2203–14.
79. Kukowska-Latallo J, Bielinska A, Johnson J, Spindler R, Tomalia D, Baker JJ. Efficient transfer of genetic material into mammalian cells using Starburst polyamidoamine dendrimers. Proc Natl Acad Sci USA. 1996;93:4897–902.
80. Okuda T, Sugiyama A, Niidome T, Aoyagi H. Characters of dendritic poly(L-lysine) analogues with the terminal lysines replaced with arginines and histidines as gene carriers *in vitro*. Biomaterials. 2004;25:537–44.
81. Radu D, Lai C, Jeftinija K, Rowe E, Jeftinija S, Lin V. A polyamidoamine dendrimer-capped mesoporous silica nanosphere-based gene transfection reagent. J Am Chem Soc. 2004;126:13216–7.
82. Haensler J, Szoka FJ. Polyamidoamine cascade polymers mediate efficient transfection of cells in culture. Bioconjug Chem. 1993;4:372–9.
83. Nishikawa M, Takakura Y, Hashida M. Pharmacokinetic evaluation of polymeric carriers. Adv Drug Deliv Rev. 1996;21:135–55.
84. Takakura Y, Hashida M. Macromolecular carrier systems for targeted drug delivery: pharmacokinetic considerations on biodistribution. Pharm Res. 1996;13:820–31.
85. Brenner B, Hostetter T, Humes H. Glomerular permselectivity: barrier function based on discrimination of molecular size and charge. Am J Physiol. 1978;234:F455–60.
86. Gerlowski L, Jain R. Physiologically based pharmacokinetic modeling: principles and applications. J Pharm Sci. 1983;72:1103–27.
87. Rennke H, Patel Y, Venkatachalam M. Glomerular filtration of proteins: clearance of anionic, neutral, and cationic horseradish peroxidase in the rat. Kidney Int. 1978;13:278–88.
88. Nishida K, Mihara K, Takino T, Nakane S, Takakura Y, Hashida M, *et al.* Hepatic disposition characteristics of electrically charged macromolecules in rat *in vivo* and in the perfused liver. Pharm Res. 1991;8:437–44.
89. Takakura Y, Fujita T, Furitsu H, Nishikawa M, Sekaki H, Hashida M. Pharmacokinetics of succinylated proteins and dextran sulfate in mice: implications for hepatic targeting of protein drugs by direct succinylation via scavenger receptors. Int J Pharm. 1994;105:19–29.
90. Dr O, Opsonization PN. biodistribution, and pharmacokinetics of polymeric nanoparticles. Int J Pharm. 2006;307:93–102.
91. D'Souza AJ, Topp EM. Release from polymeric prodrugs: linkages and their degradation. J Pharm Sci. 2004;93:1962–79.
92. Hunt CA, MacGregor RD, Siegel RA. Engineering targeted *in vivo* drug delivery. I. the physiological and physicochemical principles governing opportunities and limitations. Pharm Res. 1986;3:333–44.
93. Khandare J, Kolhe P, Pillai O, Kannan S, Lieh-Lai M, Kannan R. Synthesis, cellular transport, and activity of polyamidoamine dendrimer-methylprednisolone conjugates. Bioconjug Chem. 2005;16:330–7.
94. Khan M, Nigavekar S, Minc L, Kariapper M, Nair B, Lesniak W, *et al. In vivo* biodistribution of dendrimers and dendrimer nanocomposites – implications for cancer imaging and therapy. Technol Cancer Res Treat. 2005;4:603–13.
95. Kaminskas L, Boyd B, Karellas P, Henderson S, Giannis M, Krippner G, *et al.* Impact of surface derivatization of poly-L-lysine dendrimers with anionic arylsulfonate or succinate groups on intravenous pharmacokinetics and disposition. Mol Pharm. 2007;4:949–61.
96. Wang S, Brechbiel M, Wiener E. Characteristics of a new MRI contrast agent prepared from polypropyleneimine dendrimers, generation 2. Invest Radiol. 2003;38:662–8.
97. Weiner EC, Brechbiel MW, Brothers H, Magin RL, Gansow OA, Tomalia DA, *et al.* Dendrimer-based metal chelates: a new class of magnetic resonance imaging contrast agents. Magn Reson Med. 1994;31:1–8.
98. Kobayashi H, Sato N, Hiraga A, Saga T, Nakamoto Y, Ueda H, *et al.* 3D-micro-MR angiography of mice using macromolecular MR contrast agents with polyamidoamine dendrimer core with reference to their pharmacokinetic properties. Magn Reson Med. 2001;45:454–60.
99. Kobayashi H, Kawamoto S, Saga T, Sato N, Hiraga A, Konishi J, *et al.* Micro-MR angiography of normal and intratumoral vessels in mice using dedicated intravascular MR contrast agents with high generation of polyamidoamine dendrimer core: reference to pharmacokinetic properties of dendrimer-based MR contrast agents. J Magn Reson Imaging. 2001;14:705–13.

100. Bryant LJ, Jordan E, Bulte J, Herynek V, Frank J. Pharmacokinetics of a high-generation dendrimer-Gd-DOTA. Acad Radiol. 2002;9:S29–33.
101. Bohrer M, Deen W, Robertson C, Troy J, Brenner B. Influence of molecular configuration on the passage of macromolecules across the glomerular capillary wall. J Gen Physiol. 1979;74:583–93.
102. Sarin H, Kanevsky A, Wu H, Sousa A, Wilson C, Aronova M, *et al.* Physiologic upper limit of pore size in the blood-tumor barrier of malignant solid tumors. J Transl Med. 2009;7:51.
103. Kobayashi H, Kawamoto S, Choyke P, Sato N, Knopp M, Star R, *et al.* Comparison of dendrimer-based macromolecular contrast agents for dynamic micro-magnetic resonance lymphangiography. Magn Reson Med. 2003;50:758–66.
104. Kobayashi H, Kawamoto S, Bernardo M, Brechbiel M, Knopp M, Choyke P. Delivery of gadolinium-labeled nanoparticles to the sentinel lymph node: comparison of the sentinel node visualization and estimations of intra-nodal gadolinium concentration by the magnetic resonance imaging. J Control Release. 2006;111:343–51.
105. Kobayashi H, Kawamoto S, Jo S, Bryant HJ, Brechbiel M, Star R. Macromolecular MRI contrast agents with small dendrimers: pharmacokinetic differences between sizes and cores. Bioconjug Chem. 2003;14:388–94.
106. Margerum LD, Campion BK, Koo M, Shargill N, Lai J-J, Marumoto A, *et al.* Gadolinium(III)DO3A macrocycles and polyethylene glycol coupled to dendrimers: Effect of molecular weight on physical and biological properties of macromolecular magnetic resonance imaging contrast agents. J Alloys Compd. 1997;249:185–90.
107. Sakharov D, Jie A, Bekkers M, Emeis J, Rijken D. Polylysine as a vehicle for extracellular matrix-targeted local drug delivery, providing high accumulation and long-term retention within the vascular wall. Arterioscler Thromb Vasc Biol. 2001;21:943–8.
108. Wiwattanapatapee R, Carreño-Gómez B, Malik N, Duncan R. Anionic PAMAM dendrimers rapidly cross adult rat intestine *in vitro*: a potential oral delivery system? Pharm Res. 2000;17:991–8.
109. Kitchens K, Kolhatkar R, Swaan P, Ghandehari H. Endocytosis inhibitors prevent poly(amidoamine) dendrimer internalization and permeability across Caco-2 cells. Mol Pharm. 2008;5:364–9.
110. Nigavekar S, Sung L, Llanes M, El-Jawahri A, Lawrence T, Becker C, *et al.* ^{3}H dendrimer nanoparticle organ/tumor distribution. Pharm Res. 2004;21:476–83.
111. Uehara T, Ishii D, Uemura T, Suzuki H, Kanei T, Takagi K, *et al.* Gamma-Glutamyl PAMAM dendrimer as versatile precursor for dendrimer-based targeting devices. Bioconjug Chem. 2010;21:175–81.
112. Kitchens K, Kolhatkar R, Swaan P, Eddington N, Ghandehari H. Transport of poly(amidoamine) dendrimers across Caco-2 cell monolayers: Influence of size, charge and fluorescent labeling. Pharm Res. 2006;23:2818–26.
113. Parrott M, Benhabbour S, Saab C, Lemon J, Parker S, Valliant J, *et al.* Synthesis, radiolabeling, and bio-imaging of high-generation polyester dendrimers. J Am Chem Soc. 2009;131:2906–16.
114. Kobayashi H, Kawamoto S, Saga T, Sato N, Hiraga A, Ishimori T, *et al.* Positive effects of polyethylene glycol conjugation to generation-4 polyamidoamine dendrimers as macromolecular MR contrast agents. Magn Reson Med. 2001;46:781–8.
115. Zhu S, Hong M, Tang G, Qian L, Lin J, Jiang Y, *et al.* Partly PEGylated polyamidoamine dendrimer for tumor-selective targeting of doxorubicin: the effects of PEGylation degree and drug conjugation style. Biomaterials. 2010;31:1360–71.
116. Kaminskas L, Boyd B, Karellas P, Krippner G, Lessene R, Kelly B, *et al.* The impact of molecular weight and PEG chain length on the systemic pharmacokinetics of PEGylated poly l-lysine dendrimers. Mol Pharm. 2008;5:449–63.
117. Kaminskas L, Wu Z, Barlow N, Krippner G, Boyd B, Porter C. Partly-PEGylated Poly-L-lysine dendrimers have reduced plasma stability and circulation times compared with fully PEGylated dendrimers. J Pharm Sci. 2009;98:3871–5.
118. Gillies E, Fréchet J. Designing macromolecules for therapeutic applications: polyester dendrimer-poly(ethylene oxide) "bow-tie" hybrids with tunable molecular weight and architecture. J Am Chem Soc. 2002;124:14137–46.
119. Venturoli D, Rippe B. Ficoll and dextran *vs.* globular proteins as probes for testing glomerular permselectivity: effects of molecular size, shape, charge, and deformability. Am J Physiol Renal Physiol. 2005;288:F605–13.
120. Lim J, Guo Y, Rostollan C, Stanfield J, Hsieh J, Sun X, *et al.* The role of the size and number of polyethylene glycol chains in the biodistribution and tumor localization of triazine dendrimers. Mol Pharm. 2008;5:540–7.
121. 2Hoppe C, Lee Y. The binding and processing of mannose-bovine serum albumin derivatives by rabbit alveolar macrophages. Effect of the sugar density. J Biol Chem. 1983;258:14193–9.
122. Yeeprae W, Kawakami S, Yamashita F, Hashida M. Effect of mannose density on mannose receptor-mediated cellular uptake of mannosylated O/W emulsions by macrophages. J Control Release. 2006;114:193–201.
123. Wijagkanalan W, Kawakami S, Takenaga M, Igarashi R, Yamashita F, Hashida M. Efficient targeting to alveolar macrophages by intratracheal administration of mannosylated liposomes in rats. J Control Release. 2008;125:121–30.
124. Barth R, Adams D, Soloway A, Alam F, Darby M. Boronated starburst dendrimer-monoclonal antibody immunoconjugates: evaluation as a potential delivery system for neutron capture therapy. Bioconjug Chem. 1994;5:58–66.
125. Barth R, Yang W, Adams D, Rotaru J, Shukla S, Sekido M, *et al.* Molecular targeting of the epidermal growth factor receptor for neutron capture therapy of gliomas. Cancer Res. 2002;62:3159–66.
126. Yang W, Barth R, Wu G, Kawabata S, Sferra T, Bandyopadhyaya A, *et al.* Molecular targeting and treatment of EGFRvIII-positive gliomas using boronated monoclonal antibody L8A4. Clin Cancer Res. 2006;12:3792–802.
127. Konda S, Wang S, Brechbiel M, Wiener E. Biodistribution of a 153 Gd-folate dendrimer, generation = 4, in mice with folate-receptor positive and negative ovarian tumor xenografts. Invest Radiol. 2002;37:199–204.
128. Yao Z, Zhang M, Sakahara H, Saga T, Arano Y, Konishi J. Avidin targeting of intraperitoneal tumor xenografts. J Natl Cancer Inst. 1998;90:25–9.
129. Wilbur D, Pathare P, Hamlin D, Buhler K, Vessella R. Biotin reagents for antibody pretargeting. 3. Synthesis, radioiodination, and evaluation of biotinylated starburst dendrimers. Bioconjug Chem. 1998;9:813–25.
130. Kobayashi H, Kawamoto S, Saga T, Sato N, Ishimori T, Konishi J, *et al.* Avidin-dendrimer-(1B4M-Gd)(254): a tumor-targeting therapeutic agent for gadolinium neutron capture therapy of intraperitoneal disseminated tumor which can be monitored by MRI. Bioconjug Chem. 2001;12:587–93.
131. Kobayashi H, Kawamoto S, Star R, Waldmann T, Brechbiel M, Choyke P. Activated clearance of a biotinylated macromolecular MRI contrast agent from the blood pool using an avidin chase. Bioconjug Chem. 2003;14:1044–7.
132. Dijkgraaf I, Rijnders A, Soede A, Dechesne A, van Esse G, Brouwer A, *et al.* Synthesis of DOTA-conjugated multivalent cyclic-RGD peptide dendrimers via 1, 3-dipolar cycloaddition and their biological evaluation: implications for tumor targeting and tumor imaging purposes. Org Biomol Chem. 2007;5:935–44.
133. Almutairi A, Rossin R, Shokeen M, Hagooly A, Ananth A, Capoccia B, *et al.* Biodegradable dendritic positron-emitting

nanoprobes for the noninvasive imaging of angiogenesis. Proc Natl Acad Sci USA. 2009;106:685–90.
134. Huang R, Qu Y, Ke W, Zhu J, Pei Y, Jiang C. Efficient gene delivery targeted to the brain using a transferrin-conjugated polyethyleneglycol-modified polyamidoamine dendrimer. FASEB J. 2007;21:1117–25.
135. Mamede M, Saga T, Ishimori T, Higashi T, Sato N, Kobayashi H, *et al.* Hepatocyte targeting of 111In-labeled oligo-DNA with avidin or avidin-dendrimer complex. J Control Release. 2004;95:133–41.
136. Kukowska-Latallo J, Raczka E, Quintana A, Chen C, Rymaszewski M, Baker JJ. Intravascular and endobronchial DNA delivery to murine lung tissue using a novel, nonviral vector. Hum Gene Ther. 2000;11:1385–95.
137. Sato N, Kobayashi H, Saga T, Nakamoto Y, Ishimori T, Togashi K, *et al.* Tumor targeting and imaging of intraperitoneal tumors by use of antisense oligo-DNA complexed with dendrimers and/or avidin in mice. Clin Cancer Res. 2001;7:3606–12.
138. Vinter-Jensen L, Frøkiaer J, Jørgensen P, Marqversen J, Rehling M, Dajani E, *et al.* Tissue distribution of 131I-labelled epidermal growth factor in the pig visualized by dynamic scintigraphy. J Endocrinol. 1995;144:5–12.
139. Yang W, Barth R, Adams D, Ciesielski M, Fenstermaker R, Shukla S, *et al.* Convection-enhanced delivery of boronated epidermal growth factor for molecular targeting of EGF receptor-positive gliomas. Cancer Res. 2002;62:6552–8.
140. Bai S, Thomas C, Ahsan F. Dendrimers as a carrier for pulmonary delivery of enoxaparin, a low-molecular weight heparin. J Pharm Sci. 2007;96:2090–106.
141. Menjoge A, Navath R, Asad A, Kannan S, Kim C, Romero R, *et al.* Transport and biodistribution of dendrimers across human fetal membranes: implications for intravaginal administration of dendrimer-drug conjugates. Biomaterials. 2010;31:5007–21.
142. Wijagkanalan W, Higuchi Y, Kawakami S, Teshima M, Sasaki H, Hashida M. Enhanced anti-inflammation of inhaled dexamethasone palmitate using mannosylated liposomes in an endotoxin-induced lung inflammation model. Mol Pharmacol. 2008;74:1183–92.
143. Wijagkanalan W, Kawakami S, Higuchi Y, Yamashita F, Hashida M. Intratracheally instilled mannosylated cationic liposome/NFkappaB decoy complexes for effective prevention of LPS-induced lung inflammation. J Control Release. 2010 in press.
144. McLennan DN, Porter CJH, Charman SA. Subcutaneous drug delivery and the role of the lymphatics. Drug Discov Today Tech. 2005;2:89–96.
145. Kaminskas L, Kota J, McLeod V, Kelly B, Karellas P, Porter C. PEGylation of polylysine dendrimers improves absorption and lymphatic targeting following SC administration in rats. J Control Release. 2009;140:108–16.
146. Florence A, Hussain N. Transcytosis of nanoparticle and dendrimer delivery systems: evolving vistas. Adv Drug Deliv Rev. 2001;50:S69–89.
147. Florence A, Sakthivel T, Toth I. Oral uptake and translocation of a polylysine dendrimer with a lipid surface. J Control Release. 2000;65:253–9.
148. Ke W, Zhao Y, Huang R, Jiang C, Pei Y. Enhanced oral bioavailability of doxorubicin in a dendrimer drug delivery system. J Pharm Sci. 2008;97:2208–16.
149. Zolnik B, Sadrieh N. Regulatory perspective on the importance of ADME assessment of nanoscale material containing drugs. Adv Drug Deliv Rev. 2009;61:422–7.
150. Herborn C, Barkhausen J, Paetsch I, Hunold P, Mahler M, Shamsi K, *et al.* Coronary arteries: contrast-enhanced MR imaging with SH L 643A–experience in 12 volunteers. Radiology. 2003;229:217–23.
151. McCarthy T, Karellas P, Henderson S, Giannis M, O'Keefe D, Heery G, *et al.* Dendrimers as drugs: discovery and preclinical and clinical development of dendrimer-based microbicides for HIV and STI prevention. Mol Pharm. 2005;2:312–8.
152. Patton D, Cosgrove Sweeney Y, McCarthy T, Hillier S. Preclinical safety and efficacy assessments of dendrimer-based (SPL7013) microbicide gel formulations in a nonhuman primate model. Antimicrob Agents Chemother. 2006;50:1696–700.
153. Rupp R, Rosenthal S, Stanberry L. VivaGel (SPL7013 Gel): a candidate dendrimer–microbicide for the prevention of HIV and HSV infection. Int J Nanomedicine. 2007;2:561–6.
154. Yao H, Veine D, Fay K, Staszewski E, Zeng Z, Livant D. The PHSCN dendrimer as a more potent inhibitor of human breast cancer cell invasion, extravasation, and lung colony formation. Breast Cancer Res Treat. 2010 in press.
155. Kobayashi H, Sato N, Saga T, Nakamoto Y, Ishimori T, Toyama S, *et al.* Monoclonal antibody-dendrimer conjugates enable radiolabeling of antibody with markedly high specific activity with minimal loss of immunoreactivity. Eur J Nucl Med. 2000;27:1334–9.
156. Carney P, Rogers P, Johnson D. Dual isotope study of iodine-125 and indium-111-labeled antibody in athymic mice. J Nucl Med. 1989;30:374–84.
157. Casas A, Battah S, Di Venosa G, Dobbin P, Rodriguez L, Fukuda H, *et al.* Sustained and efficient porphyrin generation *in vivo* using dendrimer conjugates of 5-ALA for photodynamic therapy. J Control Release. 2009;135:136–43.
158. Chauhan A, Jain N, Diwan P, Khopade A. Solubility enhancement of indomethacin with poly(amidoamine) dendrimers and targeting to inflammatory regions of arthritic rats. J Drug Target. 2004;12:575–83.
159. Chauhan A, Diwan P, Jain N, Tomalia D. Unexpected *in vivo* anti-inflammatory activity observed for simple, surface functionalized poly(amidoamine) dendrimers. Biomacromolecules. 2009;10:1195–202.
160. Cheng Y, Man N, Xu T, Fu R, Wang X, Wen L. Transdermal delivery of nonsteroidal anti-inflammatory drugs mediated by polyamidoamine (PAMAM) dendrimers. J Pharm Sci. 2007;96:595–602.
161. Vandamme T, Brobeck L. Poly(amidoamine) dendrimers as ophthalmic vehicles for ocular delivery of pilocarpine nitrate and tropicamide. J Control Release. 2005;102:23–38.
162. Bhadra D, Bhadra S, Jain N. PEGylated peptide dendrimeric carriers for the delivery of antimalarial drug chloroquine phosphate. Pharm Res. 2006;23:623–33.
163. Koyama Y, Talanov V, Bernardo M, Hama Y, Regino C, Brechbiel M, *et al.* A dendrimer-based nanosized contrast agent dual-labeled for magnetic resonance and optical fluorescence imaging to localize the sentinel lymph node in mice. J Magn Reson Imaging. 2007;25:866–71.
164. Subbarayan M, Shetty SJ, Srivastava TS, Noronha OP, Samuel AM, Mukhtar H. Water-soluble 99mTc-labeled dendritic novel porphyrins tumor imaging and diagnosis. Biochem Biophys Res Commun. 2001;281:32–6.
165. Zhang Y, Sun Y, Xu X, Zhang X, Zhu H, Huang L, *et al.* Synthesis, biodistribution, and microsingle photon emission computed tomography (SPECT) imaging study of technetium-99m labeled PEGylated dendrimer poly(amidoamine) (PAMAM)-folic acid conjugates. J Med Chem. 2010;53:3262–72.
166. Sarin H, Kanevsky A, Wu H, Brimacombe K, Fung S, Sousa A, *et al.* Effective transvascular delivery of nanoparticles across the blood-brain tumor barrier into malignant glioma cells. J Transl Med. 2008;6:80.